CHEMISTRY
A EUROPEAN JOURNAL

DOI: 10.1002/chem.201001256

Heterometallic Modular Metal–Organic 3D Frameworks Assembled via New Tris-β-Diketonate Metalloligands: Nanoporous Materials for Anion Exchange and Scaffolding of Selected Anionic Guests

Lucia Carlucci,* Gianfranco Ciani, Simona Maggini, Davide M. Proserpio, and Marco Visconti[a]

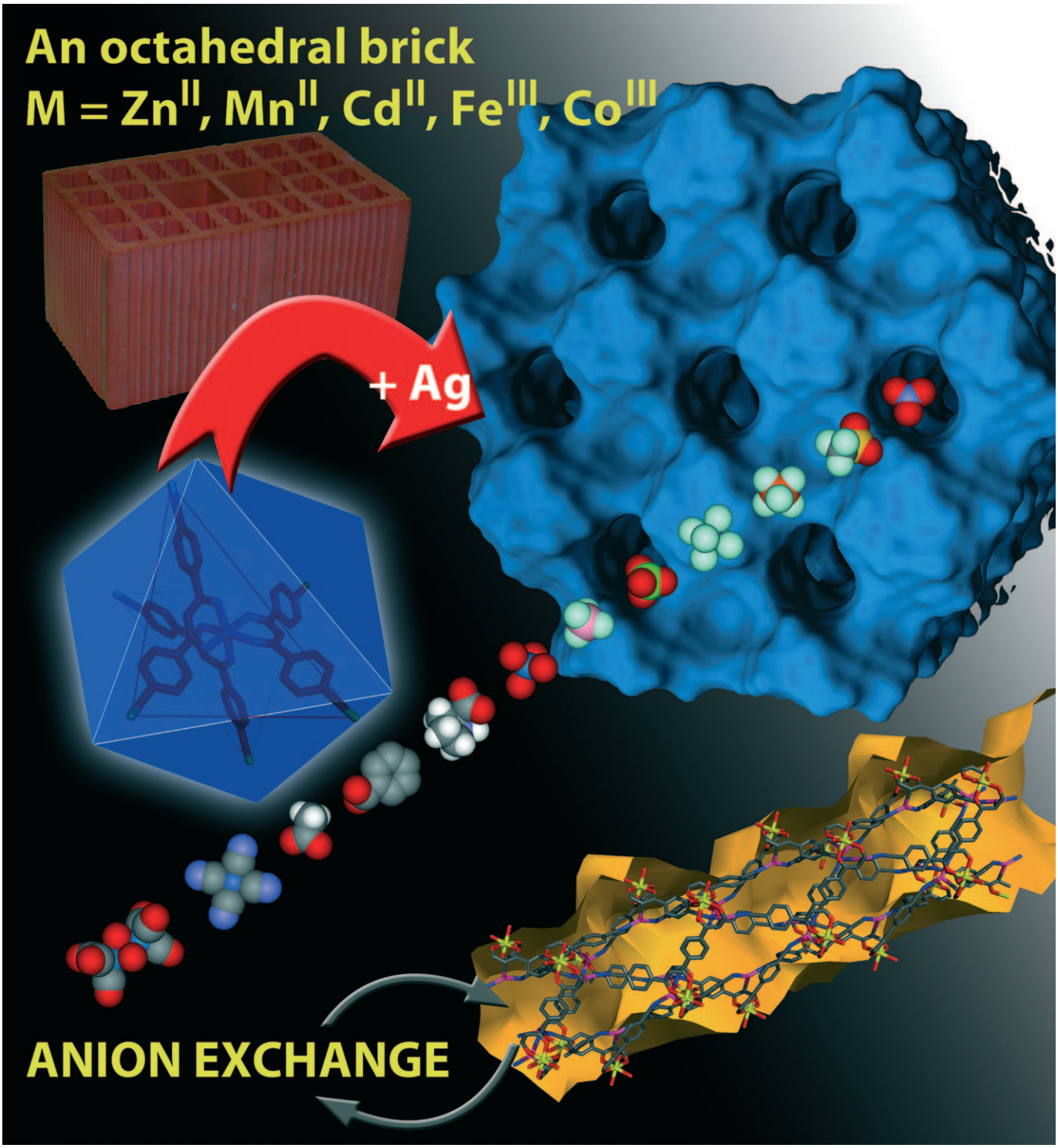

Abstract: The modular engineering of heterometallic nanoporous metal–organic frameworks (MOFs) based on novel tris-chelate metalloligands, prepared using the functionalised β-diketone 1,3-bis(4′-cyanophenyl)-1,3-propanedione (**HL**), is described. The complexes $[M^{III}\mathbf{L}_3]$ ($M=Fe^{3+}$, Co^{3+}) and $[M^{II}\mathbf{L}_3](NEt_4)$ ($M=Mn^{2+}$, Co^{2+}, Zn^{2+}, Cd^{2+}) have been synthesised and characterised, all of which exhibit a distorted octahedral chiral structure. The presence of six *exo*-oriented cyano donor groups on each complex makes it a suitable building block for networking through interactions with external metal ions. We have prepared two families of MOFs by reacting the metalloligands $[M^{III}\mathbf{L}_3]$ and $[M^{II}\mathbf{L}_3]^-$ with many silver salts AgX ($X=NO_3^-$, BF_4^-, PF_6^-, AsF_6^-, SbF_6^-, $CF_3SO_3^-$, tosylate), specifically the $[M^{III}\mathbf{L}_3Ag_3]X_3$·Solv and $[M^{II}\mathbf{L}_3Ag_3]X_2$·Solv network species. Very interestingly, all of these network species exhibit the same type of 3D structure and crystallise in the same trigonal space group with similar cell parameters, in spite of the different metal ions, ionic charges and X^- counteranions of the silver salts. We have also succeeded in synthesising trimetallic species such as $[Zn_xFe_y\mathbf{L}_3Ag_3](ClO_4)_{(2x+3y)}$·Solv and $[Zn_xCd_y\mathbf{L}_3Ag_3](ClO_4)_2$·Solv (with $x+y=1$). All of the frameworks can be described as sixfold interpenetrated **pcu** nets, considering the Ag^+ ions as simple digonal spacers. Each individual net is homochiral, containing only Δ or Λ nodes; the whole array contains three nets of type Δ and three nets of type Λ. Otherwise, taking into account the presence of weak Ag–C σ bonds involving the central carbon atoms of the β-diketonate ligands of adjacent nets, the six interpenetrating **pcu** networks are joined into a unique non-interpenetrated six-connected frame with the rare **acs** topology. The networks contain large parallel channels of approximate hexagonal-shaped sections that represent 37–48% of the cell volume and include the anions and many guest solvent molecules. The guest solvent molecules can be reversibly removed by thermal activation with retention of the framework structure, which proved to be stable up to about 270°C, as confirmed by TGA and powder XRD monitoring. The anions could be easily exchanged in single-crystal to single-crystal processes, thereby allowing the insertion of selected anions into the framework channels.

Keywords: anions · coordination polymers · heterometallic complexes · ion exchange · metalloligands · metal–organic frameworks · polymers

Introduction

Open metal–organic frameworks (MOFs)[1,2] are considered as promising materials for many potential applications, such as gas storage, molecular sensing, separation, ion exchange, catalysis, optics, magnetism and others,[2] and great attention is currently focused on their design. A useful approach to the rational synthesis of such network species involves the use of molecular building blocks, usually metal-containing species called metalloligands,[3–6] that have suitably oriented peripheral *exo* donor groups and are therefore able to direct the formation of the polymeric array. The metalloligands are used in place of organic ligands to join different metal centres, thus possibly affording heterobimetallic architectures (including many 3d–4f systems)[4] with additional properties. In contrast to the secondary building units (SBUs) that can be envisaged as fundamental constituent units of the networks assembled by the reticular chemistry approach,[1b,c,7] the metalloligands are distinct entities in their own right. This stepwise approach implies the initial careful selection of the polyfunctional ligands to be employed in the preparation of the discrete metal–organic building blocks with the desired geometry. Chelating ligands are the most frequently used, which generate bis- or tris-chelated complexes and contain additional outward directed donor groups (typically carboxylate, nitrile or pyridyl). For instance, tris(dipyrrinato) metal complexes[5] have been shown to be a versatile class of metalloligands for the preparation of a variety of interesting MOF structures. A few functionalised β-diketonate ligands have also been employed as suitable chelating agents for the preparation of metalloligands; the known examples include tris-chelated complexes with 3-substituted acetylacetonates (having pyridyl or CN substituent groups)[6a,b] and the bis-chelated species $[Cu(pyac)_2]$ (pyac = 3-(4-pyridyl)pentane-2,4-dionato).[6c,d]

We report here an approach for the modular engineering of heterometallic MOFs based on the use of a functionalised β-diketone, namely 1,3-bis(4′-cyanophenyl)-1,3-propanedione (**HL**).

The corresponding β-diketonate ligand ($\mathbf{L}^-$; Scheme 1), besides acting as a chelating agent towards a metal centre, can coordinate other metals through the two CN groups, and can potentially also interact with metals through its central carbon atom. We have employed this ligand to prepare novel neutral tris-chelate complexes of metal trications $[M\mathbf{L}_3]$ ($M=Co^{III}$, Fe^{III}) and anionic tris-chelate complexes of metal dications $[M\mathbf{L}_3]^-$ ($M=Mn^{II}$, Co^{II}, Zn^{II}, Cd^{II}). These discrete metal–organic building blocks have been used in the construction of heterometallic MOFs by reaction with a

[a] Dr. L. Carlucci, Prof. Dr. G. Ciani, Dr. S. Maggini, Prof. Dr. D. M. Proserpio, M. Visconti
Dipartimento di Chimica Strutturale e Stereochimica Inorganica
Università degli Studi di Milano
Via Venezian 21, 20133 Milano (Italy)
Fax: (+39) 0250314454
E-mail: lucia.carlucci@unimi.it

Supporting information for this article is available on the WWW under http://dx.doi.org/10.1002/chem.201001256.

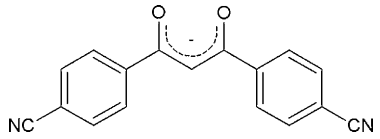

Scheme 1. 1,3-Bis(4′-cyanophenyl)-1,3-propanedionato ($\mathbf{L}^-$).

number of silver salts AgX ($X = NO_3^-$, BF_4^-, PF_6^-, AsF_6^-, SbF_6^-, $CF_3SO_3^-$, tosylate). We have thereby obtained numerous representatives of a family of three-dimensional (3D) nanoporous networks in crystalline form with the compositions $[M^{III}\mathbf{L}_3Ag_3]X_3\cdot$Solv and $[M^{II}\mathbf{L}_3Ag_3]X_2\cdot$Solv, and these have been structurally characterised. Surprisingly, all of these networks exhibit a very similar structure, thus indicating a great efficiency of the metalloligands together with the Ag^+ spacers in orienting the relevant polymeric architecture. The results of our investigations on the network porosity and on the anion-exchange ability of these materials, which contain large 1D parallel channels that allow the insertion of interesting anionic species, are also reported.

Results and Discussion

Stepwise modular synthesis: We started with the aim of synthesising a new tris-chelate metalloligand, containing six *exo*-oriented donor groups, as a building block for heterometallic networks. For this purpose, we selected as ligand a symmetrically disubstituted β-diketonate anion, considering the successful use of such species in the preparation of metalloligands.[6] We synthesised the 1,3-bis(4′-cyanophenyl)-1,3-propanedione (**HL**) molecule, which, to the best of our knowledge, has not hitherto been employed in the context of metal coordination polymers (but has been used in the preparation of some palladium complexes with liquid-crystal properties).[8] It was prepared according to a literature method,[9] using a base-catalyzed condensation between 4-acetylbenzonitrile and methyl 4-cyanobenzoate. Single crystals of **HL** were obtained and investigated by X-ray diffraction. The crystal structure is comprised of flat molecules in the enol form, with intramolecular H-bonding (see Figure S1 and Table S1 in the Supporting Information).

The corresponding β-diketonate ligand ($\mathbf{L}^-$) can serve both as a chelating agent towards a metal centre and as a donor towards other external metals through the two *exo*-directed cyano groups; moreover, at the same time, it can also potentially interact outwards with other metal atoms through the central carbon atom of the β-diketonate, as already observed in many dinuclear and oligonuclear complex species.[10] The $\mathbf{L}^-$ anion was subsequently reacted with metal ions to afford the tris-chelate metalloligands.

The metalloligands: Deprotonation of **HL** with NEt_4OH in ethanol or water afforded solutions of the salt $(NEt_4)\mathbf{L}$, which could then be reacted with metal ions M^{3+} or M^{2+}. Bulk polycrystalline products were obtained for the tris-chelate complexes of both trications $[M^{III}\mathbf{L}_3]$ ($M = Fe^{3+}$ (**1a**), Co^{3+} (**1b**)) and dications $[M^{II}\mathbf{L}_3](NEt_4)$ ($M = Mn^{2+}$ (**2a**), Co^{2+} (**2b**), Zn^{2+} (**2c**), Cd^{2+} (**2d**)). The metalloligands were characterised by IR and ^{1}H NMR spectroscopy, powder XRD, thermogravimetric analysis (TGA) and selected magnetic measurements. Attempts to obtain the Fe^{2+} species failed, most probably due to partial oxidation of the metal ions under the reaction conditions.

To fully characterise these species, we attempted to grow single crystals from the crude materials using slow-diffusion methods. For the neutral species $[M^{III}\mathbf{L}_3]$, this was a difficult task since crystallisation is highly dependent on the solvent system, producing only polycrystalline samples that exhibit a variety of powder XRD patterns. In the case of $[Fe\mathbf{L}_3]$, however, a crystalline product was obtained in methanol that corresponded to the dinuclear Fe^{III} species $[Fe\mathbf{L}_2(\mu\text{-OMe})]_2$ (as evidenced by single-crystal X-ray analysis; see Figure S2 in the Supporting Information). We serendipitously isolated single crystals of the acetone-solvated species $[Co\mathbf{L}_3]$ (**1b**), the crystal structure of which is reported herein. On the other hand, we have been able to obtain good yields of single crystals of all of the $[M^{II}\mathbf{L}_3](NEt_4)$ metalloligands (**2a–d**), which exhibit very similar triclinic unit cells (see Table S1 in the Supporting Information) in spite of the presence of different guest solvent molecules.

The crystal structure of **1b**·3(acetone) is built-up by the packing of discrete neutral $[Co\mathbf{L}_3]$ molecules, as illustrated in Figure 1 (top). It can be compared with the structure of the THF-solvated metalloligand **2b**, $[Co\mathbf{L}_3](NEt_4)\cdot$THF, taken as representative of the anionic tris-chelate species (Figure 1, bottom).

All of these metalloligands exhibit a distorted octahedral chiral structure (of ideal D_3 symmetry; see the selected bond parameters in Table S2 in the Supporting Information) and are packed in centrosymmetric space groups, thus resulting in a balance of the Δ and Λ enantiomeric forms. On comparing the MO_6 coordination geometries, we observe that the M–O bond lengths show the expected trends, that is, longer bonds on going from the first to the second transition row (e.g., Zn^{2+} vs. Cd^{2+} 2.054(2)–2.118(2) Å vs. 2.242(2)–2.278(2) Å) and shorter bonds with increased metal charge (e.g., Co^{2+} vs. Co^{3+} 2.047(3)–2.088(3) Å vs. 1.884(3)–1.893(3) Å).

The orientations of the six cyano donor groups in each metalloligand are approximately those required for a six-connected octahedral node in the networking process (for instance, the M···N distances and N···M···N angles for **1b** are in the ranges 9.316(5)–9.374(6) Å and 86.04(4)–98.18(4)° (cisoid angles) and 173.43(4)–173.85(4)° (transoid angles); on the other hand, for **2b**, the corresponding interactions span the intervals 9.424(7)–9.550(5) Å and 67.50(6)–127.21(6)° (cisoid angles) and 163.94(6)–172.14(5)° (transoid angles), with much larger deviations from the ideal angular values).

We have also prepared and structurally characterised crystals of a Cd^{2+} metalloligand with a quite different countercation, specifically the salt $[Cd\mathbf{L}_3](PPN)$ (PPN = bis(triphe-

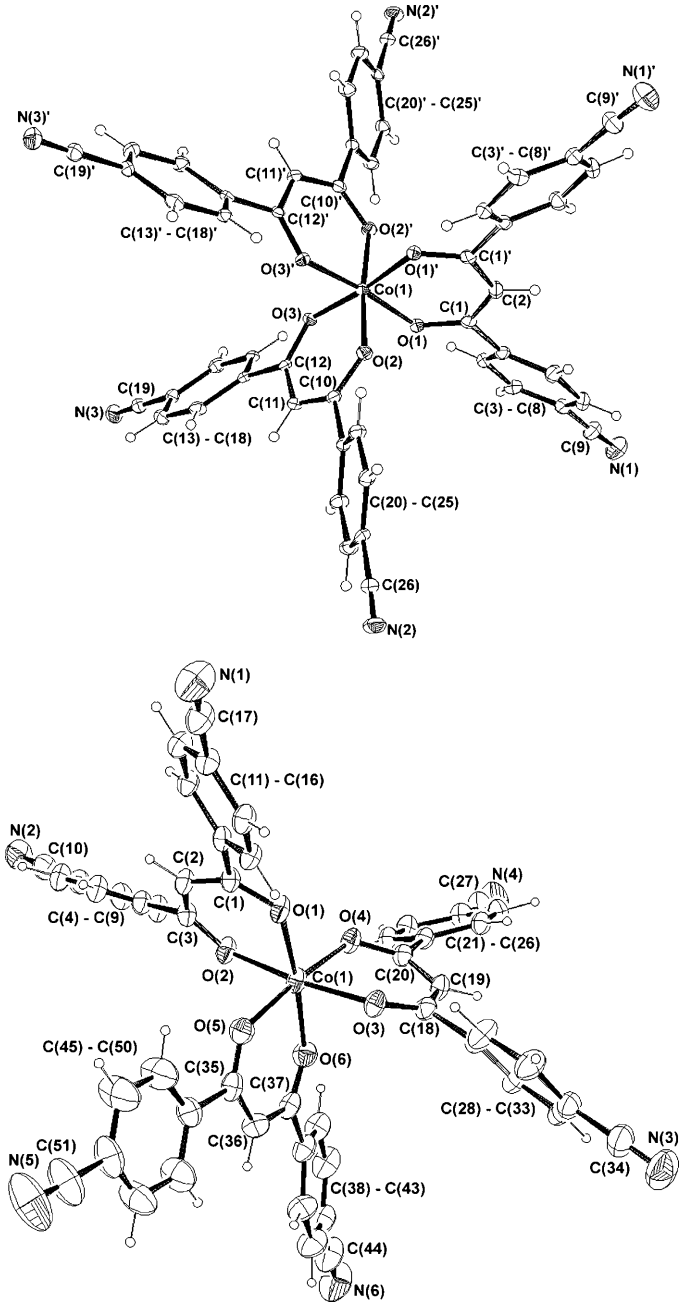

Figure 1. ORTEP drawings of the metalloligands Δ-[$Co^{III}\mathbf{L}_3$] (**1b**) (top) and Λ-$[Co^{II}\mathbf{L}_3]^-$ (**2b**) (bottom). Data were collected at 150 K and 293 K, respectively. Thermal ellipsoids are drawn at the 30% probability level.

nylphosphine)iminium) (**2d′**) (see Tables S1 and S2 in the Supporting Information) to ascertain a possible templating role of the cation in the subsequent step of the self-assembly of the 3D heterometallic network (see below).

The heterometallic MOFs: Reactions of the metalloligands, both the M^{III}- and the M^{II}-containing complexes, with many different AgX salts in appropriate solvents afforded crystalline products of $[M^{III}\mathbf{L}_3Ag_3]X_3$·Solv (**3**) and $[M^{II}\mathbf{L}_3Ag_3]X_2$·Solv (**4**) network species, respectively. Most of these products proved suitable for single-crystal X-ray analysis, though in some cases the crystallographic data were of poor quality due to significant disorder of the guest solvent molecules and of the counteranions X^- that populate the large network channels (see below).

Within the family $[M^{III}\mathbf{L}_3Ag_3]X_3$·Solv (**3**), we have investigated crystals of the species **3a** ($M=Fe^{3+}$; $X^-=CF_3SO_3^-$), **3b** ($M=Fe^{3+}$; $X^-=PF_6^-$), **3c** ($M=Fe^{3+}$; $X^-=BF_4^-$), **3d** ($M=Fe^{3+}$; $X^-=ClO_4^-$), **3e** ($M=Co^{3+}$; $X^-=SbF_6^-$), **3f** ($M=Co^{3+}$; $X^-=CF_3SO_3^-$) and **3g** ($M=Co^{3+}$; $X^-=BF_4^-$), but only the structures of **3a** and **3b** are reported here in full detail. The structure of **3a** was selected as being representative of this family of networks.

A more extensive series of members of the family $[M^{II}\mathbf{L}_3Ag_3]X_2$·Solv (**4**) was isolated as single crystals, specifically: **4a** ($M=Mn^{2+}$; $X^-=BF_4^-$), **4b** ($M=Zn^{2+}$; $X^-=BF_4^-$), **4c** ($M=Zn^{2+}$; $X^-=ClO_4^-$), **4d** ($M=Zn^{2+}$; $X^-=CF_3SO_3^-$), **4e** ($M=Zn^{2+}$; $X^-=PF_6^-$), **4f** ($M=Zn^{2+}$; $X^-=AsF_6^-$), **4g** ($M=Zn^{2+}$; $X^-=SbF_6^-$), **4h** ($M=Zn^{2+}$; $X^-=NO_3^-$), **4i** ($M=Zn^{2+}$; $X^-=$tosylate), **4j** ($M=Cd^{2+}$; $X^-=ClO_4^-$) and **4k** ($M=Cd^{2+}$; $X^-=BF_4^-$). The structures of **4b**, **4c**, **4e**, **4i**, **4j** and **4k** have been fully refined, while for the remainder we determined only the cell parameters. The structure of **4c** was selected as being representative of family **4**.

Attempts to react the Co^{2+} metalloligand (**2b**) with different silver salts did not produce crystals of the corresponding network species because of cobalt oxidation accompanied by Ag^+ reduction to the metal under the reaction conditions employed, as evidenced by the formation of a silver mirror on the walls of the reaction vessel.

All of the crystals of the families **3** and **4** belong to the trigonal system, space group $P\bar{3}$ (no. 147), with similar unit-cell parameters (see Table 1 and Tables S3 and S5 in the Supporting Information), and their structures contain a very similar complex 3D network, based on the $M\mathbf{L}_3$ metalloligands as six-connected nodes, since they use all of their six *exo*-oriented cyano functionalities to bind six Ag^+ ions.

The nearly octahedral geometry and the bond parameters of the free metalloligands are essentially retained in the nodes of the networks with only some minor changes (see Table S4 in the Supporting Information), with values in accordance with the trends outlined above. The metal ions lie on threefold crystallographic axes and the M–O bond lengths are in the ranges 1.980(4)–1.998(4) Å for Fe^{III}, 2.037(3)–2.084(3) Å for Zn^{II} and 2.225(8)–2.268(4) Å for Cd^{II}.

The silver ions can be considered as digonal spacers that link the metal complexes to generate a 3D network, which exhibits the **pcu** (point symbol $4^{12}.6^3$) topology (as exemplified in the case of compound **4c** in Figure 2). The "cubic" cages are strongly distorted towards rhombohedral shape because of a stretching along one of the body diagonals, that is, that aligned in the direction of the crystallographic *c*-axis, which is of length $3\times c$ (long body diagonal 49.45 Å vs. short diagonals 35.03 Å in **4c**).

The edges of the cages in families **3** and **4** have lengths in the range 22.46–22.97 Å and the cage M···M···M acute angles span the interval 68.64–74.08° (see Table 1).

Table 1. Comparison of the crystallographic data and the network parameters (in the **pcu** and **acs** topologies) for the refined MOFs.

	Crystal data					**pcu** topology				**acs** topology		
MOF	*a* [Å]	*c* [Å]	*c*/*a*	*V* [Å^3]	% void[a]	edge [Å]	long diag. [3×*c*] [Å]	short diag. [Å]	M···M···M[b] acute angles [°]	d_1,d_2[c] [Å]	d_3[c] [Å]	Ag–C [Å]
3a	15.217(1)	16.738(2)	1.100	3356.4(5)	43.9	22.621	50.214	34.733	71.26	13.787 10.703	15.217	2.827
3b	14.620(7)	17.046(1)	1.166	3155.4(4)	37.6	22.457	51.138	33.846	68.64	13.362 10.769	14.620	3.831
4b	15.733(3)	16.486(6)	1.048	3534(2)	47.3	22.788	49.458	35.523	73.44	14.005 10.791	15.733	2.474
4c	15.457(1)	16.483(3)	1.066	3410.5(7)	44.9	22.597	49.449	35.034	72.65	13.916 10.646	15.457	2.468
4e	15.458(1)	16.524(2)	1.069	3419.4(5)	45.5	22.627	49.571	35.055	72.55	13.882 10.694	15.458	2.479
4i	15.649(6)	16.472(8)	1.053	3493(2)	47.5	22.720	49.416	35.368	73.24	13.973 10.743	15.649	2.451
4j	15.824(3)	16.563(6)	1.047	3592(2)	47.4	22.970	49.689	35.720	73.49	14.075 10.852	15.824	2.531
4k	15.939(2)	16.463(5)	1.033	3622(1)	47.8	22.915	49.389	35.878	74.08	14.137 10.841	15.939	2.515
4l	15.808(1)	16.582(2)	1.049	3588.8(4)	47.9	22.910	49.747	35.701	73.39	14.100 10.833	15.808	2.490
5b	15.613(1)	16.477(3)	1.055	3478.3(7)	46.2	22.699	49.431	35.306	73.12	13.979 10.715	15.613	2.472

[a] Values computed with the program Platon after removing the clathrate solvent and anion molecules. [b] M refers to the central metal atom of the corresponding SBU. [c] d_1, d_2 and d_3 represent the M···M distances between the central metal atoms of adjacent SBUs.

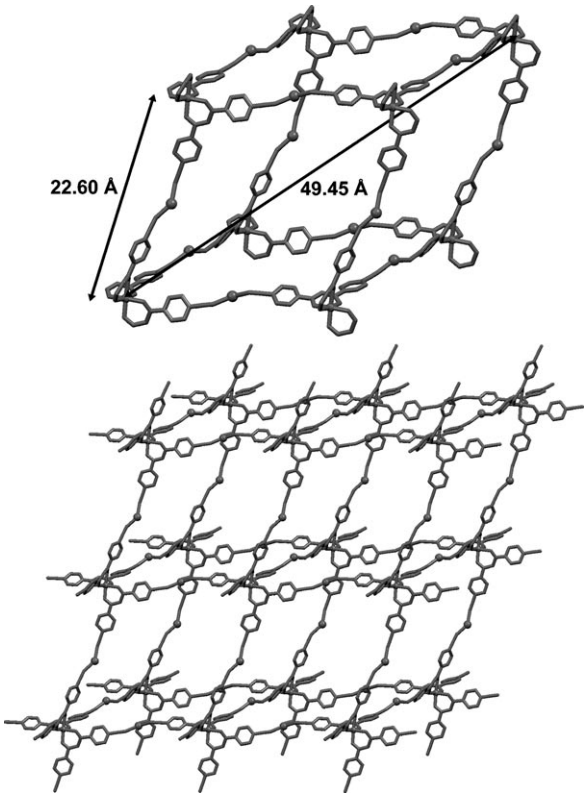

Figure 2. View of a single "cubic" cage (top) and of the **pcu** network (bottom) in **4c**.

The networks are sixfold interpenetrated (see Figure 3) and each individual net is homochiral, comprised of exclusively Δ or Λ tris-chelate metal nodes. The whole array contains a group of three nets of type Δ and an enantiomeric group of three nets of type Λ; within each group the three nets are related by pure translation (translational vector [100] and its symmetry equivalents), while the two groups have a centrosymmetric relationship (3Δ+3Λ), as shown in Figure 4. This type of interpenetration is classified as belonging to Class IIIa [$Z=6(3*2)$], whereby both translational and non-translational symmetry operations correlate the six nets.[11]

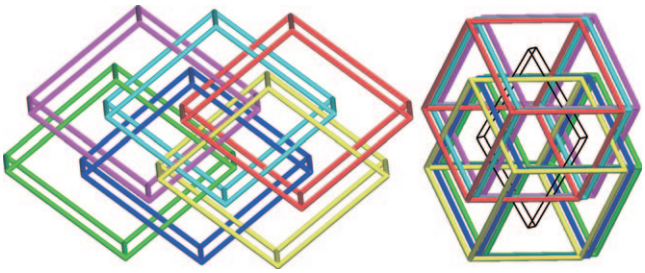

Figure 3. Two schematic views of the sixfold interpenetrated **pcu** networks showing that the 6 nets are grouped by 3+3, with the 3 nets in each set related by translation: Class IIIa [$Z=6(3*2)$].

These networks represent the first example of sixfold interpenetration for **pcu** topology and as such are unprecedented for this topology. Previous examples of highly interpenetrating **pcu** nets have comprised only two cases of fourfold[12] and two cases of fivefold interpenetration.[13]

A more rigorous analysis of the differences within the network structures of families **3** and **4** reveals a very interesting feature. In all of the networks formed by the anionic metalloligands, $[M^{II}\mathbf{L}_3Ag_3]X_2$·Solv (**4**), the silver spacers significantly interact with the central carbon atoms of the β-di-

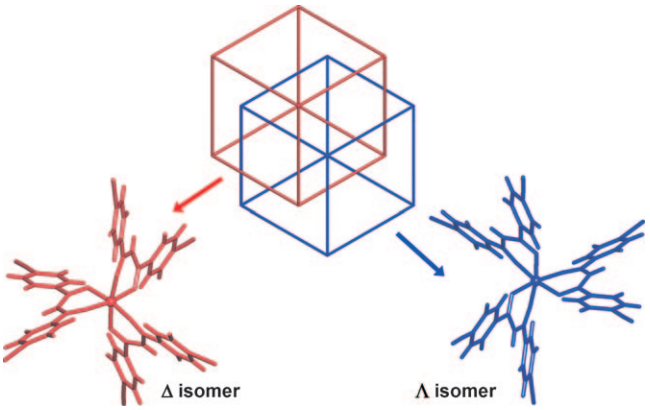

Figure 4. Schematic view down the *c*-axis of the sixfold interpenetration, evidencing the two centrosymmetrically related homochiral groups (3Δ+3Λ).

ketonate ligands, chelating the metal nodes of adjacent nets. All of the silver atoms and all of the β-diketonate ligands are involved in these weak Ag–C σ bonds (in the range 2.451(11)–2.531(7) Å; see Figure 5 and Table 1). Similar rel-

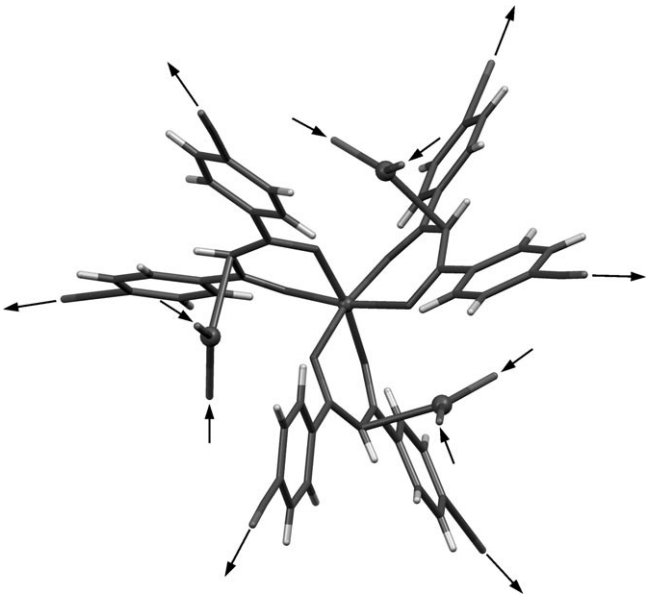

Figure 5. Interactions of the metalloligand node with three Ag atoms of three adjacent nets. This [M**L**$_3$Ag$_3$] moiety is a novel SBU that presents six donor cyano groups and six acceptor sites on the silver atoms (see arrows).

atively weak bonds between Ag and methine C atoms have previously been observed in many β-diketonate oligomeric complexes,[14] which, however, exhibit shorter Ag–C contacts, as short as 2.24 Å in the anion [Pd$_2$Ag(acac)$_2$-(C$_6$F$_5$)$_4$]$^-$.[14b] On the other hand, in the networks derived from the neutral metalloligands, [M^{III}**L**$_3$Ag$_3$]X$_3$·Solv (**3**), these Ag···C interactions are either markedly weaker (e.g., 2.827(7) Å in **3a**) or become non-existent (e.g., a shortest Ag···C(methine) contact of 3.831(7) Å in **3b**), probably due to the lack of a negative charge on the metal complex.

The coordination of the Ag atoms (Ag–N bonds in the range 2.114(7)–2.217(7) Å) generally shows marked deviations from linearity (with N-Ag-N angles in the range 140.8(2)–154.3(3)°). The bending is most probably due to the weak Ag···C and/or Ag···anion interactions and this can introduce a certain flexibility of the frameworks.

Each chiral node (Δ or Λ) interacts with three silver atoms belonging to three adjacent **pcu** nets of opposite chirality. Taking into account these additional interactions, the six interpenetrating **pcu** nets are bundled into a unique non-interpenetrated six-connected network with the rare **acs** topology.[11b,15] The [M**L**$_3$Ag$_3$] moiety can be considered as a novel six-connected SBU (see Figure 5) that generates the whole 3D network (schematically illustrated in Figure 6),

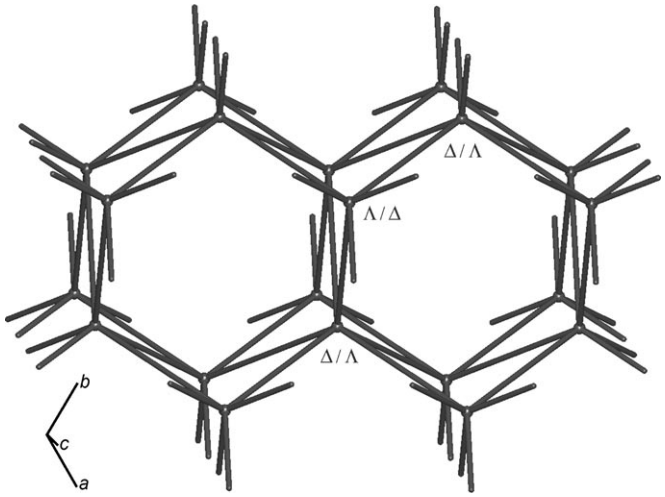

Figure 6. Schematic depiction of the six-connected **acs** network; the alternation of the Δ and Λ nodes is shown.

which exhibits trigonal prismatic nodes, whereby all of the edges are double-stranded edges (see Figure 7) and the M···M contacts are about half the length of the edges in the **pcu** networks. The [M**L**$_3$Ag$_3$] SBU uses all six cyano donor groups and the three Ag atoms (each accepting two external CN) to form the single network. These twelve interactions of the SBU (six as donor and six as acceptor) give rise to the double-edged single **acs** net. It may also be noted that the chirality of each node of the net is opposite to that of the six nodes connected to it.

Within the double edges (illustrated in Figure 7), weak π-π interactions are observed involving the phenyl rings of different diketonate ligands. Geometrical data for the prismatic nodes are reported in Table 1.

The **acs** topology (point symbol ($4^9.6^6$)) applies to a network formed by linking trigonal prisms, as observed in tungsten carbide, WC.[15] It is a uninodal edge-transitive net (one kind of node and one kind of edge). Some examples of **acs** networks in coordination polymers have been previously characterised.[15b,16]

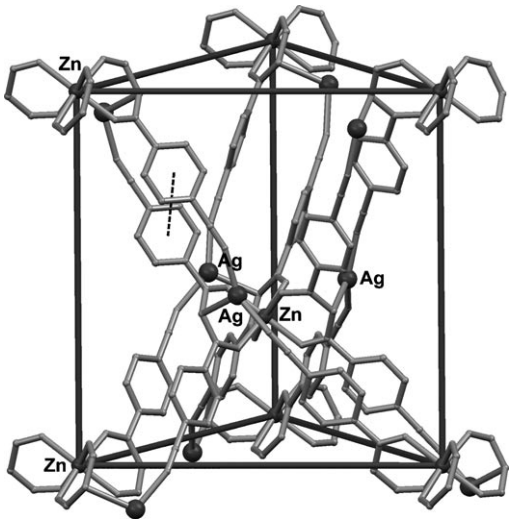

Figure 7. The trigonal-prismatic environment of each node in **4c**, representative of the family **4**, showing the double-edges with π–π interactions. The three upper edges are longer (Zn···Zn 13.916 Å) than the three lower ones (Zn···Zn 10.646 Å). A dotted line shows one of the π–π interactions involving the phenyl rings (for **4c**: 0°/3.57 Å/1.66 Å/angle/distance/offset between phenyl rings).

The most interesting feature of these species (families **3** and **4**) is the fact that only one network structure type is always obtained, in spite of the different metal ions, their ionic charges and the nature of the X^- counteranions of the silver salts, thus indicating a great efficiency of the selected metalloligands together with the Ag spacers in orienting the final polymeric architecture. This target topology is strictly determined by the rigid geometry of the molecular building blocks. Thus, it can be anticipated that other members of the families **3** and **4** might be obtained by changing the M^{III} or M^{II} metals.

To confirm this exceptional network preference, we carried out further experiments. We investigated the possible role of the countercation of the anionic metalloligands in driving the formation of the MOFs. After the preparation and the single-crystal X-ray characterisation of the species $[Cd\mathbf{L}_3](PPN)$ (PPN = bis(triphenylphosphine)iminium) (**2d′**, see Table S1 in the Supporting Information), containing a bulky cation, we reacted it with $AgClO_4$ under the same conditions as previously used for networking, and obtained the species $[Cd\mathbf{L}_3Ag_3](ClO_4)_2$·Solv (**4j′**), which proved to be isostructural with **4j**. Again, we observed that the change of a factor that might have had a drastic effect on the resulting framework had no effect within these species.

It therefore seemed reasonable to expect that analogous MOFs containing mixed network nodes might be obtained by subjecting different metalloligands to the same reaction. We succeeded in synthesising the trimetallic species $[Zn_xFe_y\mathbf{L}_3Ag_3](ClO_4)_{(2x+3y)}$·Solv (**5a**) and $[Zn_xCd_y\mathbf{L}_3Ag_3](ClO_4)_2$·Solv (**5b**) (both with $x+y=1$). By means of SEM equipped for elemental analysis, we confirmed in both cases the presence of the three metals in approximately the correct ratios. The two compounds were found to display crystal cell parameters similar to those found for families **3** and **4** belonging to the same space group. The structure of **5b** was successfully refined with a statistical distribution of Zn and Cd atoms at the network nodes (i.e., $x=y=0.5$; see Table S3 in the Supporting Information). The M–O bond lengths (2.111(4)–2.160(4) Å) were found to be intermediate between the Zn–O (2.037(3)–2.084(4) Å) and Cd–O (2.225(8)–2.268(4) Å) bond lengths observed in the Zn^{II} and Cd^{II} networks of family **4**.

Channel structure and nanoporous behaviour: In contrast to the well-established structural features of the networks, the content of the large intra-framework void spaces is much less easily understood due to marked disorder of the included species, as is often the case in nanoporous network polymers. Indeed, these void regions represent a large part of the cell volume and are mainly localised in large parallel channels of an almost hexagonal-shaped section, all running along the *c*-axis direction (see Figure 8). They contain the anions (often disordered and in some cases weakly interacting with the Ag^+ ions), as well as the clathrate solvent molecules (mixtures of solvents), which are generally disordered. Though the data collections were performed at $T=150$ K, these molecules could not be located from the X-ray crystallographic data. A single channel of **4c** is illustrated in Figure 9.

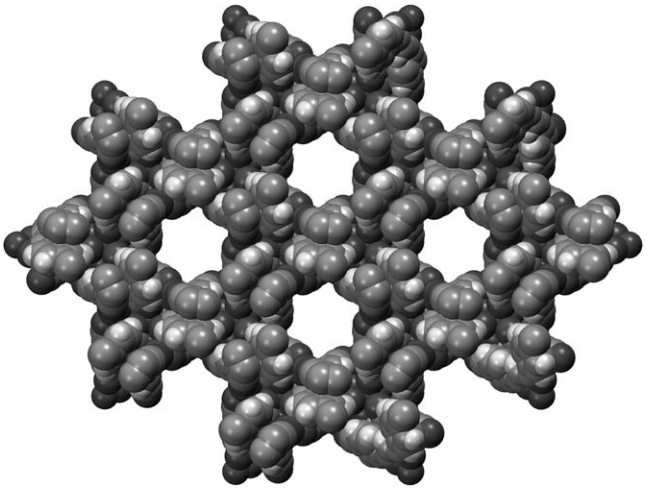

Figure 8. View of the packing down the *c*-axis in **4c** showing the channels of approximate hexagonal section.

The dimensions of the channels are determined by the mutual positions of the SBUs: as in the prototypical structure of WC, with the **acs** topology, the channels are columns of stacked trigonal antiprismatic cages (as shown schematically in Figure 10).

The lengths of the M···M edges are reported in Table 1, specifically those of the d_1, d_2 and d_3 edges (shown in Figure 10). Comparison shows that the networks are rather flexible (breathing nets have recently been defined as "soft

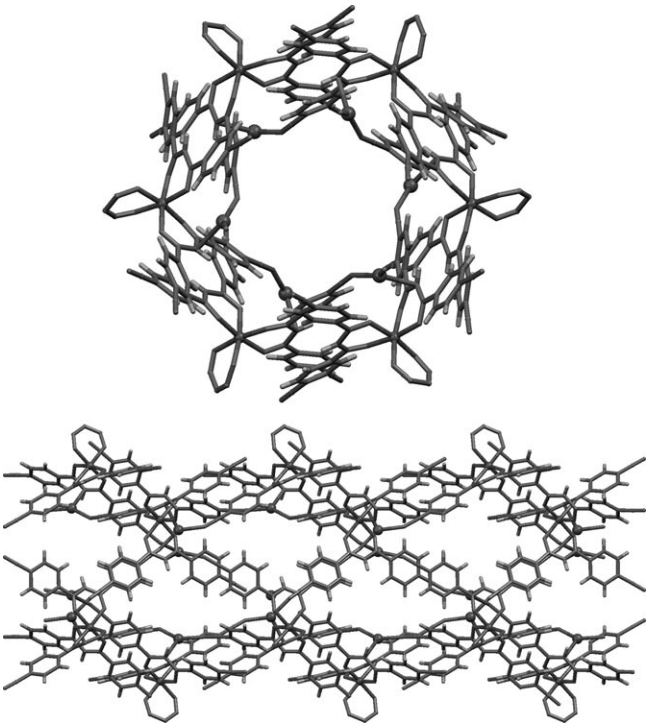

Figure 9. Front (top) and side (bottom) views of a single channel in **4c**.

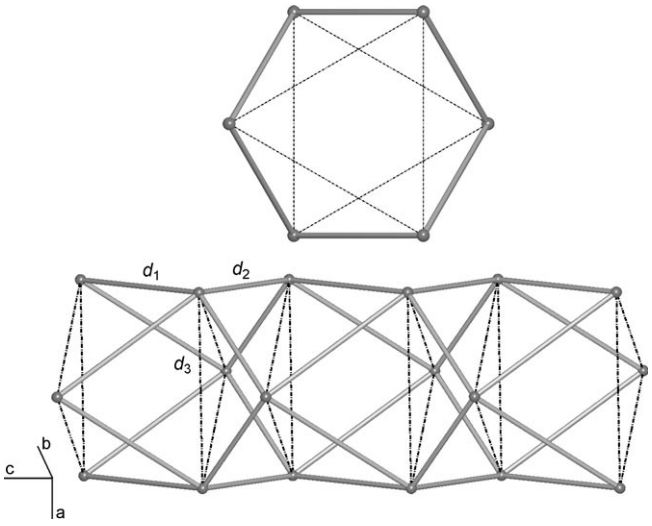

Figure 10. Schematic illustration of the network channels according to the **acs** topology: front (top) and side (bottom) views.

porous networks"),[17] especially because of the flexible linkage produced by the Ag^+ ions; the geometrical variations reflect in part the nature of the nodes (of moderately increasing dimensions on going from Fe^{III} to Zn^{II} to Cd^{II}), but mainly the different contents of the channels. The cell volumes show significant differences, with values ranging from 3155.4(4) Å^3 (**3b**) to 3622(1) Å^3 (**4k**), accompanied by a decrease of the *c*/*a* ratio from 1.17 to 1.03 (see Table 1 and Table S5 in the Supporting Information).[18] This trend implies a reduction of the stretching along the *c*-direction of the channels, with an enlargement of their section (parallel to the *ab* plane). Indeed, the d_3 edges (see above) increase from 14.620 Å to 15.939 Å and the free voids from 37.5% to 47.8%.

The walls of the channels are formed by the double edges described above (see Figure 7), with the bridging Ag atoms somewhat protruding towards the interior of the channels. Thus, the walls are covered by phenyl aromatic groups of the ligands, cyano groups and Ag atoms.

The Ag atoms define the inner section of the channels and, as can be seen from the side view (Figure 9, bottom), they are disposed at the vertices of equilateral triangles with edges of about 9.53 Å in **4c**. The diameter of the largest sphere that can be contained in these channels is about 5.4 Å (as computed with the program Cavity, implemented in Platon).[19] The channels can be easily accessed and depleted, so that the guest solvent mixtures are readily lost (at least in part) upon exposure to the air; the overall composition is therefore not constant and to some extent can change with time.

Notably, the presence of low-coordinated Ag atoms on the walls of the channels, which can be considered as coordinatively unsaturated metal centres (UMCs)[3b,20] since they can adopt diverse coordination environments,[21] is of potential interest because they can significantly interact with guest molecules. Indeed, most of the cases in which anions have been better localised have shown the existence of weak Ag···anion interactions inside the channels.

Due to the fact that the guest species are severely disordered and cannot be located in the X-ray structures, the exact stoichiometries of these species are not easily determined. Also, elemental analyses are not very meaningful because the amounts of guest solvent are quite variable.

To confirm the anionic content in family **4**, we also prepared a polymeric network containing the perrhenate anion, specifically $[Cd\mathbf{L}_3Ag_3](ReO_4)_2$ (**4l**), and performed an inductively coupled plasma (ICP) analysis on crystals of this species to establish the correct stoichiometric ratio among the three metals. The results showed the Re/Cd ratio (observed value 2.2) to be essentially correct, whereas the Ag/Cd ratio (observed value 4.3) was too high. This may be attributed to the fact that metallic silver inevitably settles on the surface of the crystals, as also shown by powder XRD patterns acquired from ground crystals.[22]

Attempts to establish the nature and amount of the clathrate solvent molecules were performed by ^{1}H NMR spectroscopy of mixtures obtained by suspending weighed crystal samples of the network species in $CDCl_3$ for the time necessary to achieve equilibration. Dichloromethane, ethanol and water molecules in a variable ratio were found to fill the channels. For example, we determined for **4c** (with pentafluorotoluene as an added standard): $[Zn\mathbf{L}_3Ag_3](ClO_4)_2$-$(CH_2Cl_2)_{0.10–2.47}(EtOH)_{0.46–1.07}(H_2O)_{2.20–4.62}$.

These experiments also showed the insolubility of the crystals under these conditions. No signals of the metalloligands or free ligands were detected in $CDCl_3$ solution,

which implies that the amount of dissolved building blocks in the mother liquor was too low to be detected by NMR spectroscopy.

The amounts of clathrate solvent molecules were not constant and depended on many experimental variables (such as the ambient temperature, the time needed to isolate the crystals, and so on), evidencing that they can be very easily removed from the frameworks.

TG traces showed that the guests were completely lost in the temperature range 30–50 °C (about 10 % w/w), while the networks proved to be stable up to about 270 °C (see Figure S3 in the Supporting Information). The process is reversible in that the desolvated samples left at RT adsorbed water from the ambient atmosphere very quickly (about 6 % w/w) (see Figure S4 in the Supporting Information for compound **4c**). Moreover, during these processes the structure was retained, as evidenced by powder XRD analyses (see Figure S4 in the Supporting Information). The results showed the desolvation to be a reversible single-crystal to single-crystal process.[23a] This behaviour could be essentially ascribed to a second-generation nanoporous material with a permanent porosity, assisted by a certain network flexibility (though the possibility that the distinct interpenetrating **pcu** nets can, at least in part, moderately change their relative positions during the depletion would seem to be a feature of third-generation materials).[24] Work is in progress to evaluate the adsorption properties and selectivity of the desolvated species towards vapours and gases.

Anion exchange: The most promising property of these networks relies on their ability to exchange the anions present in their channels, taking into account the insolubility of the crystals in common solvents. Exchange experiments were performed to evaluate the preferred interactions of the frameworks with different anions. We selected as host networks the $[Zn\mathbf{L}_3Ag_3]X_2$·Solv species, specifically **4b** (X = BF_4^-), **4c** (X = ClO_4^-), **4d** (X = $CF_3SO_3^-$) and **4e** (X = PF_6^-). The exchanges were monitored by FTIR spectroscopy, optical microscopy, powder XRD spectra (see Figure 11) and single-crystal X-ray diffraction on selected compounds. Salient data are reported in Table 2.

The conclusions that could be drawn from these results were that anions can be easily exchanged in single-crystal to single-crystal processes,[23b] and some preferences could also be extracted, for example: a) nitrate and perchlorate very readily displace BF_4^-, PF_6^- and triflate anions; b) triflate is very mobile and can be substituted by the other anions; c) using PF_6^-, we can easily substitute triflate, whereas the substitution of perchlorate is only partial. As described above, the channel walls are covered by low-coordinated silver ions (UMCs) and these exposed centres can interact with anions. The preferences observed in these exchanges are thus most likely related to the greater anion coordination ability. The channel dimensions, on the other hand, are suitable for all of the exchanged anions, but the largest ones are only partially exchanged (see below). More quantitative competitive experiments are planned for future studies. Anyway, these materials seem good candidates for anion-exchange processes.

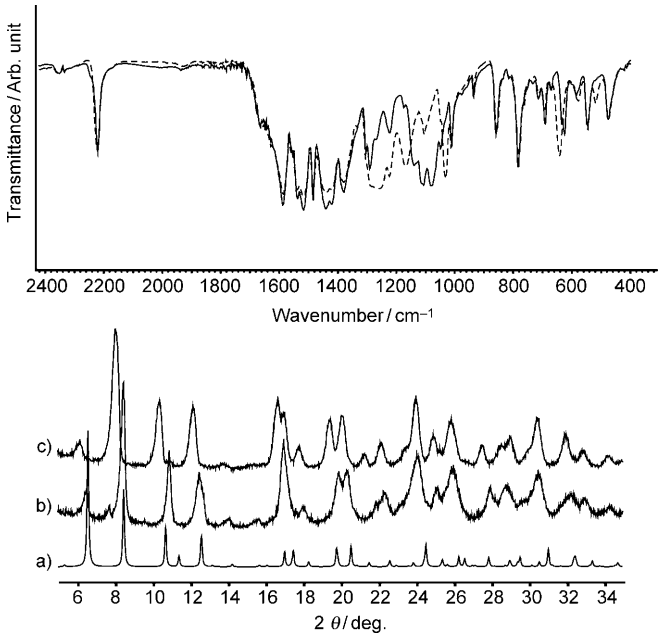

Figure 11. Top: IR spectra of an original sample of compound $[Zn^{II}\mathbf{L}_3Ag_3](CF_3SO_3)_2$ (**4d**) (dashed line) and of the same sample exchanged with $NaClO_4$ (full line). Bottom: XRPD patterns of $[Zn^{II}\mathbf{L}_3Ag_3](CF_3SO_3)_2$ (**4d**), calculated (a) and experimental (b), in comparison with that obtained after exchange with $NaClO_4$ (c).

Table 2. Inorganic anion-exchange process results.[a]

	$NaBF_4$	$NaClO_4$	$NaNO_3$	KPF_6
$[Zn^{II}\mathbf{L}_3Ag_3](\mathbf{BF_4})_2$ (**4b**)		Y (1 h)	Y (1 h)	P (24 h)
$[Zn^{II}\mathbf{L}_3Ag_3](\mathbf{ClO_4})_2$ (**4c**)	N		P (24 h)	P (27 h)
$[Zn^{II}\mathbf{L}_3Ag_3](\mathbf{CF_3SO_3})_2$ (**4d**)	Y (30 min)	Y (2 h)	Y (15 min)	Y (45 min)
$[Zn^{II}\mathbf{L}_3Ag_3](\mathbf{PF_6})_2$ (**4e**)	P (24 h)	Y (3 h)	Y (2 h)	

[a] Y = almost complete, as estimated by IR spectroscopy, P = partial, N = no exchange. In parentheses, the time of the exchange process.

Our findings that the 1D channels are easily accessible and the satisfactory results of the exchange processes with inorganic anions prompted us to try to insert some different selected anionic species. In this way, we introduced into the network different anions, including organometallic motifs, organic molecules and coordination compounds, monitoring the exchange processes by FTIR spectroscopy and the structural integrity of the crystals by powder XRD analysis. On the basis of previous exchange experiments, we selected as the starting polymer $[Zn\mathbf{L}_3Ag_3](X)_2$ with X = tetrafluoroborate (**4b**), because of the good mobility of these anions.

The exchange experiments were performed by suspending **4b** in solutions of different salts with selected anions. Perrhenate can easily displace the BF_4^- anion, and the process can be considered complete after about 1 h, as clearly

shown by IR spectroscopy monitoring (see Figure S10 in the Supporting Information). In this way, different metal-containing anions can be inserted into the network, generating new heterometallic host–guest systems.

Other exchange experiments were carried out using organometallic complex anions. The anionic dinuclear organometallic complex $[Re_2(CO)_6(\mu\text{-}OH)_3]^-$ could be introduced into the 1D channels by exchange. In this case, the exchange was slower and after 1 d it was still only partial. However, IR spectroscopy clearly indicated the presence of the carbonyl complex within the framework (see Figure S11 in the Supporting Information). Considering the large dimensions of this anion, it may be the case that it cannot diffuse into the interior of the crystal, but only into the peripheral regions. This last result opens the way to use our framework as a heterogeneous support for the immobilisation of organometallic compounds employed in homogeneous catalysis.

We attempted to insert the anion $[HFe(CO)_4]^-$ using a fourfold excess of its NEt_4^+ salt in MeOH, but the exchange was quite modest and was accompanied by some destruction of the network. On the other hand, exchange with $[Ni(CN)_4]^{2-}$ was almost complete within 3 h, but it proceeded with some structural modification, as evidenced by powder XRD. In this way, it seems that it may be possible to devise strategies for the elimination of cyano-metal complexes from solutions.

Partial exchanges were observed using sodium acetate and sodium prolinate. Finally, when the exchanges involved anions that strongly interacted with the silver atoms of the network (such as halides and pseudo-halides or BH_4^-), drastic structural changes or even framework decomposition were evident from the powder XRD spectra.

Conclusion

The well-established synthetic strategy involving the use of rigid metalloligands for the construction of a target structure, in this case heterometallic metal–organic frameworks, seemed to work well. We employed the β-diketone 1,3-bis(4′-cyanophenyl)-1,3-propanedione (**HL**) to build novel tris-chelate metalloligands $[M\mathbf{L}_3]$ ($M = Co^{III}$, Fe^{III}) and $[M\mathbf{L}_3]^-$ ($M = Mn^{II}$, Co^{II}, Zn^{II}, Cd^{II}). These are chiral octahedral building blocks with six *exo*-oriented cyano donor groups suitable for the construction of nanoporous MOFs by reaction with a number of AgX silver salts. We obtained more than twenty heterometallic networks $[M^{III}\mathbf{L}_3Ag_3]X_3\cdot Solv$ and $[M^{II}\mathbf{L}_3Ag_3]X_2\cdot Solv$, with the peculiar feature that all exhibit the same type of network structure, in spite of the different metal nodes, ionic charges and X^- counteranions. In addition, these networks represent the first example of sixfold interpenetration for the **pcu** topology, belonging to Class IIIa. The nanoporous behaviour and anion-exchange ability have been investigated and we succeeded in replacing, at least partially, the original anions in the channels with selected anionic species, such as coordination complexes and organometallic anions. The walls of the channels are covered by Ag^+ ions that can interact with the guest species.

These results are of interest both from a structural and from a functional point of view. Due to the easy reproducibility of construction of the 3D network structures, many new species based on other M^{II} and M^{III} metal ions (obtained through the synthesis of their corresponding metalloligands) can be anticipated. Mixed metalloligand frameworks can also be constructed, as we have demonstrated (with compounds **5a** and **5b**). Heteropolymetallic systems can thus, in principle, be assembled, taking further advantage of the possibility of inserting metal complexes within the array by anion-exchange processes, as we have accomplished here with the insertion of ReO_4^-, $[Re_2(CO)_6(OH)_3]^-$ and $[Ni(CN)_4]^{2-}$.

Potential applications to be considered in the future include storage and elimination from solutions of anionic metal complexes or specific organic anions and immobilisation of catalytic fragments.

Experimental Section

Reagents and general procedures: All commercial reagents and solvents employed (Sigma–Aldrich) were of high-grade purity and were used as supplied without further purification. $NEt_4[Re_2(CO)_6(OH)_3]$, $K[HFe(CO)_4]$ and $K_2[Ni(CN)_4]$ were synthesised according to literature methods.[25–27] All manipulations were performed under aerobic conditions unless standard Schlenk techniques were required. Anhydrous tetrahydrofuran was freshly distilled under nitrogen from sodium/benzophenone. NMR spectra were recorded on Bruker AC300 or AC400 instruments; δ values are given in ppm relative to tetramethylsilane. Infrared spectra were collected on a Perkin–Elmer PARAGON 1000 FTIR spectrometer equipped with an i-series FTIR microscope. Thermogravimetric analysis (TGA) was performed on a Perkin–Elmer TGA7 instrument under dynamic nitrogen (total flow rate 20 $cm^3 min^{-1}$). A ramp rate of 10 °C min^{-1} in the range 30–650 °C was used. Powder patterns were recorded on a Philips PW1820 diffractometer ($Cu_{K\alpha}$ radiation, $\lambda = 1.5405$ Å) in the 5–35° 2θ range (0.02° and 2.5 s per step). Magnetic susceptibilities (χ_M) were determined at room temperature using an MSB-AUTO (Sherwood Scientific) magnetic balance. Three measurements were performed for every sample (50–100 mg). Diamagnetic corrections were estimated from Pascal's constants. Elemental analyses were carried out at the Microanalytical Laboratory of the University of Milan. Semiquantitative scanning electron microscopy (SEM) analyses were performed with a JEOL JSM-5500LV instrument equipped with an EDS spectrometer IXRF EDS2000. The Zn/Re/Ag ratio was determined by ICP-MS (Perkin-Elmer ELAN5500) after microwave digestion of the sample in concentrated HNO_3.

1,3-Bis(4′-cyanophenyl)-1,3-propanedione (HL): Anhydrous THF (32 mL) was added under nitrogen to a dispersion of 60% NaH in mineral oil (1.3833 g, 34.58 mmol). The mixture was cooled to 0 °C, whereupon 4-acetylbenzonitrile (1.6523 g, 11.38 mmol) was added. A solution of methyl 4-cyanobenzoate (2.0131 g, 12.49 mmol) in anhydrous THF (8 mL) was then added dropwise over a period of 15 min. The pale-yellow mixture was refluxed for 16 h under nitrogen and then quenched with ice. Upon addition of 0.1 M HCl, the ligand **HL** was precipitated as a yellow solid and was recovered by filtration and washed with distilled H_2O. The filtrate was extracted with AcOEt (3×100 mL) and the collected organic phases were washed with a saturated aqueous solution of NaCl and dried over $MgSO_4$. Evaporation of the solvent under vacuum gave further **HL**. Both batches of solid were washed with hot EtOH (40 mL) to afford pure **HL** as a pale-yellow solid. Yield: 70%; ^1H NMR

(400 MHz, [D$_6$]acetone): $\delta = 8.39$ (d, 4H), 8.02 (d, 4H), 7.51 ppm (s, 1H); IR (KBr): $\tilde{\nu} = 3100$, 3068, 3052, 2920, 2854, 2230, 1616, 1590, 1542, 1490, 1448, 1292, 1222, 862, 832, 788, 544 cm^{-1}; elemental analysis calcd (%) for $C_{17}H_{10}N_2O_2$: C 74.44, H 3.67, N 10.21; found: C 74.31, H 3.58, N 10.43.

Tris[1,3-bis(4′-cyanophenyl)-1,3-propanedionato]iron(III) (1a): The ligand **HL** (315.5 mg, 1.150 mmol) was suspended in water (15 mL) and treated with 0.2 M NaOH (5.8 mL). After the addition of a solution of $FeCl_3{\cdot}6H_2O$ (103.7 mg, 0.384 mmol) in water (4 mL), the mixture was left under stirring overnight. Compound **1a** was recovered as a red solid by filtration, washed with water and dried in air. Yield: 98%; IR (KBr): $\tilde{\nu} =$ 3066, 2966, 2930, 2232, 1584, 1522, 1490, 1384, 1354, 1310, 1222, 862, 788, 546 cm^{-1}; magnetic susceptibility at 292 K: 5.71 μ_B.

Tris[1,3-bis(4′-cyanophenyl)-1,3-propanedionato]cobalt(III) (1b): The ligand **HL** (290.7 mg, 1.060 mmol) was suspended in water (15 mL) and treated with 0.2 M NaOH (5.3 mL). After the addition of a solution of $Na_3Co(NO_2)_6$ (142.7 mg, 0.353 mmol) in water (8 mL), the mixture was left under stirring for 2 h. Compound **1b** was recovered as a green solid by filtration, washed with water and dried in air. Yield: 82%; IR (KBr): $\tilde{\nu} = 3122$, 3096, 3068, 2918, 2854, 2228, 1614, 1524, 1450, 1384, 1292, 1224, 854, 788, 544 cm^{-1}.

Tetraethylammonium tris[1,3-bis(4′-cyanophenyl)-1,3-propanedionato]-manganate(II) (2a): EtOH (260 mL) and a 35% aqueous solution of NEt_4OH (754.8 mg, 1.794 mmol) were added to the ligand **HL** (401.9 mg, 1.465 mmol). After the further addition of a solution of $MnCl_2{\cdot}4H_2O$ (96.8 mg, 0.489 mmol) in EtOH (30 mL), the mixture was left under stirring for 15 h. Compound **2a** was recovered as a dark-orange solid by filtration, washed with water and dried in air. Yield: 61%; IR (KBr): $\tilde{\nu} =$ 3068, 3042, 2984, 2950, 2226, 1590, 1546, 1520, 1460, 1434, 1392, 1292, 1222, 862, 780, 550 cm^{-1}. Crystals of **2a** suitable for structural investigation were obtained after slow diffusion of *n*-hexane vapour into a solution in CH_2Cl_2 for 5 days.

Tetraethylammonium tris[1,3-bis(4′-cyanophenyl)-1,3-propanedionato]-cobaltate(II) (2b): A 35% aqueous solution of NEt_4OH (403.7 mg, 0.960 mmol) was added to a suspension of the ligand **HL** (220.8 mg, 0.805 mmol) in EtOH (134 mL). After the addition of a solution of $CoCl_2{\cdot}6H_2O$ (63.9 mg, 0.269 mmol) in EtOH (16 mL), the mixture was left under stirring for 1 h. Compound **2b** was recovered as a dark-orange solid by filtration, washed with water and dried in air. Yield: 81%; ^{1}H NMR (300 MHz, [D$_6$]acetone): $\delta = 15.55$ (br, 12H), 12.26 (br, 12H), 3.06 (br, 8H), 1.08 (br, 12H), −11.70 ppm (br, 3H); IR (KBr): $\tilde{\nu} = 3068$, 3042, 2988, 2226, 1590, 1546, 1518, 1464, 1438, 1392, 1294, 1224, 862, 768, 550 cm^{-1}. Crystals suitable for structural investigation were obtained after slow diffusion of diethyl ether vapour into a solution of **2b** in THF for 10 days.

Tetraethylammonium tris[1,3-bis(4′-cyanophenyl)-1,3-propanedionato]-zincate(II) (2c): A 35% aqueous solution of NEt_4OH (1120.6 mg, 2.663 mmol) was added to a suspension of the ligand **HL** (617.2 mg, 2.250 mmol) in EtOH (70 mL). After the addition of a solution of $ZnCl_2$ (102.9 mg, 0.755 mmol) in EtOH (5 mL), the mixture was left under stirring overnight. Compound **2c** was recovered as a yellow solid by filtration, washed with water and dried in air. Yield: 75%; ^{1}H NMR (300 MHz, [D$_6$]acetone): $\delta = 8.18$ (d, 12H), 7.77 (d, 12H), 6.72 (s, 3H), 3.52 (q, 12H), 1.43 ppm (br, 8H); IR (KBr): $\tilde{\nu} = 3068$, 3042, 2986, 2950, 2228, 1592, 1546, 1522, 1464, 1430, 1392, 1294, 1224, 862, 780, 550 cm^{-1}. Crystals suitable for structural investigation were obtained after slow diffusion of *n*-hexane vapour into a solution of **2c** in CH_2Cl_2 for 5 days.

Tetraethylammonium tris[1,3-bis(4′-cyanophenyl)-1,3-propanedionato]-cadmate(II) (2d): A 35% aqueous solution of NEt_4OH (326.4 mg, 0.776 mmol) was added to a suspension of the ligand **HL** (174.8 mg, 0.637 mmol) in EtOH (15 mL). After the addition of a solution of $CdNO_3{\cdot}4H_2O$ (65.5 mg, 0.212 mmol) in EtOH (4 mL), the mixture was left under stirring overnight. Compound **2d** was recovered as a yellow solid by filtration, washed with water and dried in air. Yield: 87%; ^{1}H NMR (300 MHz, [D$_6$]acetone): $\delta = 8.15$ (d, 12H), 7.78 (d, 12H), 6.65 (s, 3H), 3.52 (q, 8H), 1.40 ppm (t, 12H); IR (KBr): $\tilde{\nu} = 3068$, 3042, 2982, 2950, 2226, 1590, 1546, 1520, 1458, 1428, 1392, 1292, 1272, 1222, 856, 778, 548 cm^{-1}. Crystals suitable for structural investigation were obtained after diffusion of toluene into a solution of **2d** in CH_2Cl_2 for 4 days.

Bis(triphenylphosphine)iminium 1,3-bis(4′-cyanophenyl)-1,3-propanedionate (LPPN): The ligand **HL** (235.0 mg, 0.857 mmol) and 0.2 M NaOH (5.2 mL, 1.04 mmol) were mixed and stirred in distilled H_2O (30 mL) until a dense yellow liquid was obtained. A solution of bis(triphenylphosphine)iminium chloride (491.1 mg, 0.856 mmol) in MeOH/H_2O (10:3, 26 mL) was then added dropwise. The resulting solution was stirred at room temperature for 50 min and filtered to obtain a yellow solid. This solid was washed with distilled water and dried in air. Yield: 505.7 mg (0.623 mmol, 73%).

Bis(triphenylphosphine)iminium tris[1,3-bis(4′-cyanophenyl)-1,3-propanedionate]M^{II}: In a general procedure, **LPPN** (86.8 mg, 1.107 mmol) was dissolved in EtOH (10 mL) and a solution of MX_2 (11.3 mg, 0.037 mmol) in EtOH (4 mL) was added dropwise. The mixture was stirred at room temperature for 17 h and filtered to recover the desired product, which was washed with distilled water and a minimum amount of EtOH.

M = Cd (2d′): $MX_2 = Cd(NO_3)_2{\cdot}4H_2O$. Yield: 70% (yellow solid); ^{1}H NMR (300 MHz, [D$_6$]acetone): $\delta = 8.12$ (d, 12H), 7.54–7.76 (m, 30 H; PPN and 12H), 6.62 ppm (s, 3H, CH); IR (KBr): $\tilde{\nu} = 3058$, 2228, 1592, 1546, 1522, 1458, 1438, 1366, 1290, 1268, 858, 778, 544, 534 cm^{-1}. Crystals suitable for structural investigation were obtained after slow diffusion of *n*-hexane into a solution of **2d′** in CH_2Cl_2 for 8 days.

M = Zn (2c′): $MX_2 = ZnCl_2$. Yield: 87% (yellow solid); ^{1}H NMR (300 MHz, [D$_6$]acetone): $\delta = 8.15$ (d, 12H), 7.54–7.76 (m, 30 H; PPN and 12H), 6.69 ppm (s, 3H); IR (KBr): $\tilde{\nu} = 3058$, 2226, 1592, 1546, 1522, 1466, 1430, 1384, 1292, 1224, 860, 778, 544, 534 cm^{-1}.

Synthesis of {[Fe^{III}L$_3$Ag$_3$](ClO$_4$)$_3$}·Solv (3d): A typical synthesis of a member of the family **3** of MOFs is described here: compound **1a** (104.4 mg, 0.119 mmol) was dissolved in CH_2Cl_2 (40 mL) (solution A) and $AgClO_4$ (74.2 mg, 0.358 mmol) was dissolved in acetone (40 mL) (solution B). Portions of solution B (20 mL) were slowly added to solution A (20 mL) in two crystallising dishes (50 mL). Yellow microcrystalline powders were formed in about 5 days upon slow concentration of the two solutions left exposed to the air. The solid was collected on a Buchner funnel, washed with CH_2Cl_2 and dried in air to obtain pure **3d**. Yield: 84%; IR (KBr): $\tilde{\nu} = 3100$, 3081, 3054, 2260, 1581, 1536, 1489, 1414, 1353, 1284, 1229, 1131, 1063, 868, 834, 795, 618 cm^{-1}; magnetic susceptibility at 298 K: 6.03 μ_B.

Microcrystalline samples of the following polymers were obtained by using the appropriate silver salt in the procedure described above: **3a**: Yield: 82%. **3b**: Yield: 79%; IR (KBr): $\tilde{\nu} = 3100$, 3072, 3053, 2264, 1622, 1582, 1534, 1490, 1417, 1360, 1317, 1231, 1126, 1015, 858, 801, 700 cm^{-1}. **3c**: Yield: 75%, IR (KBr): $\tilde{\nu} = 3103$, 3075, 3054, 2263, 1580, 1538, 1496, 1414, 1352, 1263, 1231, 1065, 938, 803, 698, 619 cm^{-1}. Crystals of **3a–g** suitable for X-ray analyses were obtained by the slow diffusion method using solutions of the neutral monomers in CH_2Cl_2 and solutions of the appropriate silver salts in acetone.

Synthesis of {[Zn^{II}L$_3$Ag$_3$](BF$_4$)$_2$}·Solv (4b): A typical synthesis of a member of family **4** of MOFs is described here: compound **2c** (502.0 mg, 0.494 mmol) was dissolved in CH_2Cl_2 (215 mL) (solution A) and $AgBF_4$ (288.9 mg, 1.484 mmol) was dissolved in EtOH (215 mL) (solution B). Portions of solution B (20 mL) were slowly added to solution A (20 mL) in ten crystallising dishes (50 mL). Yellow microcrystalline powders were formed in about 5 days upon slow concentration of the respective solutions left exposed to the air. The solid was collected on a Buchner funnel, washed with CH_2Cl_2 and dried in air to obtain **4b**. Yield: 80.4%; IR (KBr): $\tilde{\nu} = 3098$, 2252, 1590, 1544, 1510, 1444, 1432, 1388, 1298, 1224, 1054, 858, 790, 546 cm^{-1}.

Microcrystalline samples of the following polymers were obtained by using the appropriate silver salt in the procedure described above. **4c**: Yield: 73%; IR (KBr): $\tilde{\nu} = 3096$, 3070, 2986, 2230, 1594, 1544, 1524, 1448, 1426, 1390, 1296, 1236, 1146, 1116, 1078, 862, 786, 626, 552 cm^{-1}. **4d**: Yield: 74%; IR (KBr): $\tilde{\nu} = 3072$, 2984, 2230, 1592, 1544, 1522, 1446, 1426, 1384, 1262, 858, 784, 546 cm^{-1}. **4e**: Yield: 70%; IR (KBr): $\tilde{\nu} = 3096$, 2230, 1594, 1544, 1522, 1444, 1428, 1386, 1296, 1224, 862, 786, 546 cm^{-1}. **4h**:

Yield: 83%; IR (KBr): $\tilde{\nu}$ = 3070, 2248, 2230, 1592, 1544, 1522, 1446, 1432, 1384, 1296, 1224, 858, 782, 546 cm^{-1}. **4j**: Yield: 86%. **4k**: Yield: 82%.

Crystals of **4a–k** suitable for X-ray analyses were obtained by the slow diffusion method using solutions of the anionic monomers in CH_2Cl_2 and solutions of the appropriate silver salts in EtOH.

Synthesis of $[Cd^{II}L_3Ag_3](ReO_4)_2$·Solv (4l): Crystals of **4l** suitable for X-ray analysis were obtained by layering solutions of $(NBu_4)ReO_4$ (4 equiv) and silver tetrafluoroborate (3 equiv) in EtOH onto a solution of the monomer **2d** (1 equiv) in CH_2Cl_2. Relative Cd/Re/Ag ratio determined by ICP analysis: 4.4:1:2.2 (calcd. 3:1:2). The high value for silver can be ascribed to the deposition of metallic silver on the crystal surface, as evidenced by powder XRD analysis.

Synthesis of $\{[Zn_xM_yL_3Ag_3](ClO_4)_z\}$ ($M = Cd^{II}$, $z = 2$ (5a); $M = Fe^{III}$, $z = 2x+3y$ (5b)): Crystals of **5a** and **5b** suitable for X-ray analyses were obtained by slow diffusion of an ethanolic solution of silver perchlorate into dichloromethane solutions containing equimolar amounts of monomers **2c**/**2d** and **2c**/**1a**, respectively.

Anion-exchange procedures (with $NaBF_4$, $NaClO_4$, $NaNO_3$ and KPF_6): Compounds **4b–e** (≈100 mg) were suspended in saturated solutions of $NaClO_4$, $NaNO_3$, KPF_6 or $NaBF_4$ in methanol (30 mL). The exchange processes were monitored by IR spectroscopy at regular intervals of 15 min or 1 h. Before each measurement, the sample was collected by filtration, washed with methanol and dried in air. To verify that the structure of the networks was retained during the exchange process, powder XRD spectra were recorded.

Exchange with $(NBu_4)ReO_4$: A sample of **4b** (51.1 mg) was added to a 0.050 M solution of $(NBu_4)ReO_4$ in methanol (4 mL) and the mixture was stirred at room temperature. The solid was then recovered by filtration, washed with methanol and dried in air. The exchange process was confirmed by the appearance of an absorption band at about 915 cm^{-1} in the IR spectrum due to the ReO_4^- anion and the disappearance of the broad band due to the BF_4^- anion at 1054 cm^{-1}. After 1 h, the process could be considered complete. Powder XRD analysis confirmed the integrity of the exchanged network.

Exchange with $(NEt_4)[Re_2(CO)_6(OH)_3]$: A sample of **4b** (50.0 mg) was added to a 0.034 M solution of $(NEt_4)[Re_2(CO)_6(OH)_3]$ in methanol (10 mL) and the mixture was stirred at room temperature for 1 d. The solid was then recovered by filtration, washed with methanol and dried in air. The IR spectrum of the exchanged solid showed the presence of carbonyl bands at 1998 and 1882 cm^{-1}. The IR band due to the BF_4^- anion decreased in intensity and moved from 1054 to 1084 cm^{-1}. The persistence of the bands due to the BF_4^- anion evidenced only a partial exchange process. The ν(CN) band shifted from 2252 to 2230 cm^{-1}. Powder XRD analysis confirmed the integrity of the exchanged network.

Exchange with $K_2[Ni(CN)_4]$: A sample of **4b** (81.2 mg) was added to a 0.013 M solution of $K_2[Ni(CN)_4]$ in MeOH/H_2O (2:1; 30 mL) and the mixture was stirred at room temperature for 3 h. A colour change from yellow-brown to green was observed within a few minutes. The solid was then recovered by filtration, washed with water and dried in air. The IR spectrum showed the presence of ν(CN) bands at 2238 and 2230 cm^{-1} (attributed to the network) and at 2168 cm^{-1} due to exchanged $[Ni(CN)_4]^{2-}$. An additional less intense ν(CN) band was observed at 2130 cm^{-1}, which as yet remains unassigned, although we note that the ν(CN) band of free $[Ni(CN)_4]^{2-}$ is at 2130 cm^{-1}. The absorption bands due to the BF_4^- anion disappeared, evidencing a complete exchange process. Powder XRD analysis of the exchanged solid showed some structural modifications.

To exclude a possible role of water in producing the structural modification during the exchange process, a sample of compound **4b** was left in a methanol/water mixture (2:1) for the same duration as that required for the exchange experiment; the same type of pattern as for the original **4b** was detected by powder XRD.

Exchange with KSCN: A sample of **4b** (12.6 mg) was added to a saturated solution of KSCN in methanol (4 mL) and immediately the mixture changed colour from brown to yellow. The solid was then recovered by filtration, washed with methanol and dried in air. The IR spectrum of the exchanged solid showed a band due to the presence of SCN^- at 2088 cm^{-1} and a lowering in the intensity of the bands due to the BF_4^- anion. Powder XRD analysis showed a complete transformation of the network.

Exchange with $NaBH_4$: A sample of **4b** (66.8 mg) was added to a 0.484 M solution of $NaBH_4$ in methanol (30 mL) and the mixture was stirred at room temperature. Immediately, the colour changed from brown to green. After 5 min, the solid was recovered by filtration, washed with methanol and dried in air. Powder XRD analysis showed a degradation of the network with the formation of metallic silver.

Exchange with sodium prolinate: A sample of **4b** (106.0 mg) was added to a 0.010 M solution of sodium prolinate in methanol (30 mL) (pH 8) and the mixture was stirred at room temperature for 1 h. The solid was then recovered by filtration, washed with methanol and dried in air. The IR spectrum of the exchanged solid, recovered after 1 h, showed a change in the absorption region corresponding to BF_4^-. No further changes were detected in the IR spectrum. Powder XRD analysis confirmed the integrity of the exchanged network, but some new peaks appeared. These data did not give clear evidence on the extent of the exchange process.

Exchange with sodium acetate: A sample of **4b** (106.0 mg) was added to a 0.020 M solution of sodium acetate in methanol (30 mL) and the mixture was stirred at room temperature for 3 h. The solid was then recovered by filtration, washed with methanol and dried in air. The IR spectrum of the exchanged solid showed a lowering of the intensity of the absorption bands due to the BF_4^- anion. However, the presence in the network of acetate was difficult to confirm because its bands were coincident with those of the network. The ν(CN) band shifted from 2252 to 2229 cm^{-1}. Powder XRD analysis confirmed the preservation of the network.

Analysis by ^{1}H NMR of guest solvents: Aliquots of 2,3,4,5,6-pentafluorotoluene (2 μL) were added to portions of $CDCl_3$ (0.75 mL) in NMR tubes and the ^{1}H NMR spectrum of such a solution was acquired. Crystals (5–10 mg) of compounds **4b–4e** and **4h** were removed from their mother liquors, dried on filter paper, weighed and quickly transferred to the NMR tubes. ^{1}H NMR spectra were acquired after about 3 h. No changes in the relative ratios between the signals were detected after this period. The signal at δ = 2.26 ppm due to the CH_3 group of 2,3,4,5,6-pentafluorotoluene was used as an internal standard to compute the amounts of clathrate solvents. Three experiments were performed for each sample. The formulae deduced were as follows:

$[ZnL_3Ag_3](BF_4)_2(CH_2Cl_2)_{0.36–1.00}(EtOH)_{0.87–1.20}(H_2O)_{1.93–4.52}$ (**4b**);

$[ZnL_3Ag_3](ClO_4)_2(CH_2Cl_2)_{0.10–2.47}(EtOH)_{0.46–1.07}(H_2O)_{2.20–4.62}$ (**4c**);

$[ZnL_3Ag_3](CF_3SO_3)_2(CH_2Cl_2)_{0.76}(EtOH)_{1.12–1.15}(H_2O)_{1.95–2.79}$ (**4d**);

$[ZnL_3Ag_3](PF_6)_2(CH_2Cl_2)_{0.18–0.20}(EtOH)_{0.47–1.70}(H_2O)_{0.61–1.55}$ (**4e**);

$[ZnL_3Ag_3](NO_3)_2(CH_2Cl_2)_{0.49–0.82}(EtOH)_{1.25–1.85}(H_2O)_{3.11–3.41}$ (**4h**).

Thermogravimetric analysis (TGA): TGA of compounds **4b–4e** and **4h** was performed in the range 30–650 °C. They each showed a weight loss of about 10% in the range 30–50 °C due to the desolvation process and a second weight loss of about 50% due to network decomposition that started at different temperatures for the different polymers (range 220–290 °C) (see Figure S3 in the Supporting Information). For polymer **4c**, the desolvation process was further monitored by heating two different samples to 100 °C and then cooling one of them to room temperature in air and the other under nitrogen. TG analyses of these samples heated up to 100 °C showed a weight loss of about 6% for the sample cooled in air and no weight loss for the sample cooled under nitrogen (see Figure S4 in the Supporting Information).

Crystallography: Crystal data for 1,3-bis(4′-cyanophenyl)-1,3-propanedione (**HL**) and for the metalloligands **1b**, **2b–2d** and **2d′** are listed in Table S1 (Supporting Information), whereas those for the MOFs **3a**,**b**, **4b**,**c**, **4e**, **4i–4l** and **5b** are listed in Table S3 (Supporting Information). Selected bond distances and angles are given in Tables S2 and S4 (Supporting Information). Data were collected on a Bruker APX II-CCD diffractometer using $Mo_{K\alpha}$ radiation (λ = 0.71073 Å). Empirical absorption corrections (SADABS)[28] were applied to all data. The structures were solved by direct methods (SIR97)[29] and refined by full-matrix least-squares on F^2 (SHELX-97)[30] using the WINGX interface.[31] All hydrogen atoms were placed in geometrically calculated positions and subsequently refined using a riding model with $U_{iso}(H) = 1.2\ U_{eq}(C)$, except in the case of the ligand **HL**, for which the hydrogen atoms were located

and refined. Anisotropic thermal parameters were assigned to all non-hydrogen atoms, except in certain cases. Specifically, in compound **2b** isotropic thermal parameters were assigned to the clathrate THF molecules and to the tetraethylammonium cation, whereas in compounds **3a** and **4l** they were assigned to all atoms of the anions other than the heavier ones (S and Re). The accessible free voids were calculated by PLATON.[19] Further details of the refinements of the disordered groups observed can be found in the cif file (under refine special details keyword). Crystals of **1b** and **3b** proved to be unstable, showing high decays of 24% and 12%, respectively, hence resulting in high *R* values. Except for the ligand **HL**, crystals of all monomers and polymers were unstable in air and so had to be kept under mineral oil. All tested crystals of **1b**, **2b**, **3a**,**b**, **4b**, **4c**, **4i–4l** also showed weak diffraction, hence resulting in high *R* values. All structures of polymers and $[FeL_2(\mu\text{-}OMe)]_2$ were found to contain disordered anions and solvents (such as dichloromethane, ethanol, methanol and water). When it was difficult to refine a consistent model for the solvents or the anions, their contribution was subtracted from the observed structure factors according to the BYPASS procedure,[32] as implemented in PLATON with the command SQUEEZE. In **4c**, **4k**,**l** and **5b**, the anions were refined with total occupancies of 2/3 for electroneutrality. In **4e**, only one hexafluorophosphate anion (disordered over three positions) was located. In **4j**, the perchlorate anions were refined with a constraint of a total occupancy of four perchlorate anions per unit cell (instead of eight for the two Wyckoff positions 6d and 2g) for electroneutrality. In **3b**, **4b** and **4i**, the anions were found to be strongly disordered and could not be located, so their contribution was subtracted with SQUEEZE; nonetheless, we report the anions in the formula since they are indeed present in the solid. The diagrams were produced using the ORTEP,[33] TOPOS,[34] and Mercury[35] programs. CCDC-776202–776218 contain the supplementary crystallographic data for this paper. These data can be obtained free of charge from The Cambridge Crystallographic Data Centre via www.ccdc.cam.ac.uk/data_request/cif.

Acknowledgements

This work was supported by MIUR within the projects PRIN 2006 POLYM2006: "Innovative experimental and theoretical methods for the study of crystal polymorphism—a multidisciplinary approach" and PRIN 2008 CRYSFORMS: "Design, properties and preparation of molecular crystals and co-crystals".

[1] a) M. O'Keeffe, M. Eddaoudi, H. Li, T. M. Reineke, O. M. Yaghi, *J. Solid State Chem.* **2000**, *152*, 3–20; b) M. Eddaoudi, D. B. Moler, H. Li, B. L. Chen, T. M. Reineke, M. O'Keeffe, O. M. Yaghi, *Acc. Chem. Res.* **2001**, *34*, 319–330; c) O. M. Yaghi, M. O'Keeffe, N. W. Ockwig, H. K. Chae, M. Eddaoudi, J. Kim, *Nature* **2003**, *423*, 705–714; d) B. Moulton, M. J. Zaworotko, *Chem. Rev.* **2001**, *101*, 1629–1658; e) P. J. Hagrman, D. Hagrman, J. Zubieta, *Angew. Chem.* **1999**, *111*, 2798–2848; *Angew. Chem. Int. Ed.* **1999**, *38*, 2638–2684; f) A. J. Blake, N. R. Champness, P. Hubberstey, W.-S. Li, M. A. Withersby, M. Schröder, *Coord. Chem. Rev.* **1999**, *183*, 117–138; g) G. Férey, *Chem. Soc. Rev.* **2008**, *37*, 191–214; h) S. R. Batten, R. Robson, *Angew. Chem.* **1998**, *110*, 1558–1595; *Angew. Chem. Int. Ed.* **1998**, *37*, 1460–1494; i) R. Robson, *J. Chem. Soc. Dalton Trans.* **2000**, 3735–3744; j) L. Carlucci, G. Ciani, D. M. Proserpio, *Coord. Chem. Rev.* **2003**, *246*, 247–289; k) L. Carlucci, G. Ciani, D. M. Proserpio, in *Making Crystals by Design — Methods, Techniques, and Applications: Networks, Topologies, and Entanglements* (Eds.: D. Braga, F. Grepioni), Wiley-VCH, Weinheim, **2007**, pp. 58–82.

[2] a) C. Janiak, *Dalton Trans.* **2003**, 2781–2804; b) S. L. James, *Chem. Soc. Rev.* **2003**, *32*, 276–288; c) S. Kitagawa, R. Kitaura, S. Noro, *Angew. Chem.* **2004**, *116*, 2388–2430; *Angew. Chem. Int. Ed.* **2004**, *43*, 2334–2375; d) J.-R. Li, R. J. Kuppler, H.-C. Zhou, *Chem. Soc. Rev.* **2009**, *38*, 1477–1504; e) J. Y. Lee, O. K. Farha, J. Roberts, K. A. Scheidt, S. T. Nguyen, J. T. Hupp, *Chem. Soc. Rev.* **2009**, *38*, 1450–1459; f) L. Ma, C. Abney, W. Lin, *Chem. Soc. Rev.* **2009**, *38*, 1248–1256; g) O. R. Evans, W. Lin, *Acc. Chem. Res.* **2002**, *35*, 511–522; h) D. Bradshaw, J. B. Claridge, E. J. Cussen, T. J. Prior, M. J. Rosseinsky, *Acc. Chem. Res.* **2005**, *38*, 273–282; i) D. Tanaka, S. Kitagawa, *Chem. Mater.* **2008**, *20*, 922–931; j) M. D. Allendorf, C. A. Bauer, R. K. Bhakta, R. J. T. Houk, *Chem. Soc. Rev.* **2009**, *38*, 1330–1352; k) M. Kurmoo, *Chem. Soc. Rev.* **2009**, *38*, 1353–1379; l) M. Dinca, J. R. Long, *Angew. Chem.* **2008**, *120*, 6870–6884; *Angew. Chem. Int. Ed.* **2008**, *47*, 6766–6779; m) M. J. Rosseinsky, *Microporous Mesoporous Mater.* **2004**, *73*, 15–30; n) A. N. Khlobystov, N. R. Champness, C. J. Roberts, S. J. B. Tendler, C. Thompson, M. Schröder, *CrystEngComm* **2002**, *4*, 426–431.

[3] a) S. Noro, S. Kitagawa, M. Yamashita, T. Wada, *Chem. Commun.* **2002**, 222–223; b) R. Kitaura, G. Onoyama, H. Sakamoto, R. Matsuda, S. Noro, S. Kitagawa, *Angew. Chem.* **2004**, *116*, 2738–2741; *Angew. Chem. Int. Ed.* **2004**, *43*, 2684–2687; c) S. Noro, H. Miyasaka, S. Kitagawa, T. Wada, T. Okubo, M. Yamashita, T. Mitani, *Inorg. Chem.* **2005**, *44*, 133–146; d) B. D. Chandler, A. P. Coté, D. T. Cramb, J. M. Hill, G. K. H. Shimizu, *Chem. Commun.* **2002**, 1900–1901; e) Y.-B. Dong, M. D. Smith, H.-C. zur Loye, *Angew. Chem.* **2000**, *112*, 4441–4443; *Angew. Chem. Int. Ed.* **2000**, *39*, 4271–4273; f) Y.-B. Dong, M. D. Smith, H.-C. zur Loye, *Inorg. Chem.* **2000**, *39*, 1943–1949; g) D. M. Ciurtin, M. D. Smith, H.-C. zur Loye, *Chem. Commun.* **2002**, 74–75; h) L. Carlucci, G. Ciani, F. Porta, D. M. Proserpio, L. Santagostini, *Angew. Chem.* **2002**, *114*, 1987–1991; *Angew. Chem. Int. Ed.* **2002**, *41*, 1907–1911; i) K.-T. Youm, S. Huh, Y. J. Park, S. Park, M.-G. Choi, M.-J. Jun, *Chem. Commun.* **2004**, 2384–2385; j) K.-T. Youm, M. G. Kim, J. Ko, M.-J. Jun, *Angew. Chem.* **2006**, *118*, 4107–4111; *Angew. Chem. Int. Ed.* **2006**, *45*, 4003–4007; k) L. Ming, L. Yuan, H. Li, J. Sun, *Inorg. Chem. Commun.* **2007**, *10*, 1281–1284; l) A.-L. Cheng, N. Liu, J.-Y. Zhang, E.-Q. Gao, *Inorg. Chem.* **2007**, *46*, 1034–1035; m) S.-S. Zhang, S.-Z. Zhan, M. Li, R. Peng, D. Li, *Inorg. Chem.* **2007**, *46*, 4365–4367; n) K. S. Suslick, P. Bhyrappa, J. H. Chou, M. E. Kosal, S. Nakagaki, D. W. Smithenry, S. R. Wilson, *Acc. Chem. Res.* **2005**, *38*, 283–291.

[4] a) Q.-D. Liu, J.-R. Li, S. Gao, B.-Q. Ma, Q.-Z. Zhou, K.-B. Yu, H. Liu, *Chem. Commun.* **2000**, 1685–1686; b) Y.-P. Ren, L.-S. Long, B.-W. Mao, Y.-Z. Yuan, R.-B. Huang, L.-S. Zheng, *Angew. Chem.* **2003**, *115*, 550–553; *Angew. Chem. Int. Ed.* **2003**, *42*, 532–535; c) Z. He, C. He, E.-Q. Gao, Z.-M. Wang, X.-F. Yang, C.-S. Liao, C.-H. Yan, *Inorg. Chem.* **2003**, *42*, 2206–2208; d) O. Guillou, C. Daiguebonne, M. Camara, N. Kerbellec, *Inorg. Chem.* **2006**, *45*, 8468–8470; e) Y.-G. Huang, X.-T. Wang, F.-L. Jiang, S. Gao, M.-Y. Wu, Q. Gao, W. Wei, M.-C. Hong, *Chem. Eur. J.* **2008**, *14*, 10340–10347; f) J.-X. Ma, X.-F. Huang, X.-Q. Song, L.-Q. Zhou, W.-S. Liu, *Inorg. Chim. Acta* **2009**, *362*, 3274–3278; g) J.-X. Ma, X.-F. Huang, Y. Song, X.-Q. Song, W.-S. Liu, *Inorg. Chem.* **2009**, *48*, 6326–6328.

[5] a) S. R. Halper, S. M. Cohen, *Inorg. Chem.* **2005**, *44*, 486–488; b) D. L. Murphy, M. R. Malachowski, C. F. Campana, S. M. Cohen, *Chem. Commun.* **2005**, 5506–5508; c) S. R. Halper, L. Do, J. R. Stork, S. M. Cohen, *J. Am. Chem. Soc.* **2006**, *128*, 15255–15268.

[6] a) V. D. Vreshch, A. B. Lysenko, A. N. Chernega, J. A. K. Howard, H. Krautscheid, J. Sieler, K. V. Domasevitch, *Dalton Trans.* **2004**, 2899–2903; b) A. D. Burrows, K. Cassar, M. F. Mahon, J. E. Warren, *Dalton Trans.* **2007**, 2499–2509; c) B. Chen, F. R. Fronczek, A. W. Maverick, *Chem. Commun.* **2003**, 2166–2167; d) B. Chen, F. R. Fronczek, A. W. Maverick, *Inorg. Chem.* **2004**, *43*, 8209–8211.

[7] a) N. W. Ockwig, O. Delgado-Friedrichs, M. O'Keeffe, O. M. Yaghi, *Acc. Chem. Res.* **2005**, *38*, 176–182; b) H. Furukawa, J. Kim, N. W. Ockwig, M. O'Keeffe, O. M. Yaghi, *J. Am. Chem. Soc.* **2008**, *130*, 11650–11661; c) D. J. Tranchemontagne, J. L. Mendoza-Cortes, M. O'Keeffe, O. M. Yaghi, *Chem. Soc. Rev.* **2009**, *38*, 1257–1283.

[8] V. Circu, T. J. K. Gibbs, L. Omnes, P. N. Horton, M. B. Hursthouse, B. W. Duncan, *J. Mater. Chem.* **2006**, *16*, 4316–4325.

[9] J. P. Anselme, *J. Org. Chem.* **1967**, *32*, 3716.

[10] See, for example: a) R. N. Hargreaves, M. R. Truter, *J. Chem. Soc. A* **1969**, 2282–2287; b) W. Rigby, H.-B. Lee, P. M. Bailey, J. A. McCleverty, P. M. Maitlis, *J. Chem. Soc. Dalton Trans.* **1979**, 387–394; c) U. Kölle, J. Kossakowski, G. Raabe, *Angew. Chem.* **1990**,

102, 839–840; *Angew. Chem. Int. Ed. Engl.* **1990**, *29*, 773–774; d) U. Koelle, C. Rietmann, G. Raabe, *Organometallics* **1997**, *16*, 3273–3281; e) H. K. Gupta, N. Rampersad, M. Stradiotto, M. J. McGlinchey, *Organometallics* **2000**, *19*, 184–191; f) L. E. Harrington, J. F. Britten, D. W. Hughes, A. D. Bain, J.-Y. Thepot, M. J. McGlinchey, *J. Organomet. Chem.* **2002**, *656*, 243–257; g) T. Matsumoto, D. J. Taube, R. A. Periana, H. Taube, H. Yoshida, *J. Am. Chem. Soc.* **2000**, *122*, 7414–7415; h) T. Matsumoto, R. A. Periana, D. J. Taube, H. Yoshida, *J. Mol. Catal. A* **2002**, *180*, 1–18; i) S. Patra, B. Mondal, B. Sarkar, M. Niemeyer, G. K. Lahiri, *Inorg. Chem.* **2003**, *42*, 1322–1327; j) J. Shono, Y. Nimura, T. Hashimoto, K. Shimizu, *Chem. Lett.* **2004**, *33*, 1422–1423.

[11] a) V. A. Blatov, L. Carlucci, G. Ciani, D. M. Proserpio, *CrystEngComm.* **2004**, *6*, 378–395; b) I. Baburin, V. A. Blatov, L. Carlucci, G. Ciani, D. M. Proserpio, *J. Solid State Chem.* **2005**, *178*, 2452–2474.

[12] a) B. Kesanli, Y. Cui, M. R. Smith, E. W. Bittner, B. C. Bockrath, W. Lin, *Angew. Chem.* **2005**, *117*, 74–77; *Angew. Chem. Int. Ed.* **2005**, *44*, 72–75. Here, the **pcu** description only applies if the entire polynuclear units [$Zn_4(\mu_4$-O)] are considered as nodes. b) S. Aitipamula, A. Nangia, *Chem. Commun.* **2005**, 3159–3161. Here, the **pcu** description applies if a synthon description of the H-bond is considered.

[13] a) Y.-M. Lu, Y.-Q. Lan, Y.-H. Xu, Z.-M. Su, S.-L. Li, H.-Y. Zang, G.-J. Xu, *J. Solid State Chem.* **2009**, *182*, 3105–3112; b) L. Fan, D. Xiao, E. Wang, Y. Li, Z. Su, X. Wang, J. Liu, *Cryst. Growth Des.* **2007**, *7*, 592–594. The **pcu** description only applies if the nodes are represented by polynuclear "Cd_2" units in ref. [13a] and by "Cu_6" polynuclear units in ref. [13b].

[14] a) W. H. J. Watson, C. T. Lin, *Inorg. Chem.* **1966**, *5*, 1074–1077; b) J. Fornies, R. Navarro, M. Tomas, E. P. Urriolabeitia, *Organometallics* **1993**, *12*, 940–943; c) K.-M. Chi, K.-H. Chen, S.-M. Peng, G.-H. Lee, *Organometallics* **1996**, *15*, 2575–2578; d) E. Alonso, J. Fornies, C. Fortuno, A. Martin, A. G. Orpen, *Organometallics* **2003**, *22*, 5011–5019; e) K. Akhbari, A. Morsali, *Cryst. Growth Des.* **2007**, *7*, 2024–2030.

[15] a) O. Delgado-Friedrichs, M. O'Keeffe, O. M. Yaghi, *Acta Crystallogr. Sect. A* **2003**, *59*, 515–525; b) A. C. Sudik, A. P. Cote, O. M. Yaghi, *Inorg. Chem.* **2005**, *44*, 2998–3000.

[16] a) Y. Cui, H. L. Ngo, P. S. White, W. Lin, *Chem. Commun.* **2002**, 1666–1667; b) G. Yang, R. G. Raptis, *Chem. Commun.* **2004**, 2058–2059; c) J. H. Yoon, S. B. Choi, Y. J. Oh, M. J. Seo, Y. H. Jhon, T.-B. Lee, D. Kim, S. H. Choi, J. Kim, *Catal. Today* **2007**, *120*, 324–329; d) T.-T. Luo, H.-C. Wu, Y.-C. Jao, S.-M. Huang, T.-W. Tseng, Y.-S. Wen, G.-H. Lee, S.-M. Peng, K.-L. Lu, *Angew. Chem.* **2009**, *121*, 9625–9628; *Angew. Chem. Int. Ed.* **2009**, *48*, 9461–9464; e) S. Ma, J. M. Simmons, D. Yuan, J.-R. Li, W. Weng, D. J. Liu, H.-C. Zhou, *Chem. Commun.* **2009**, 4049–4051; Y. Qiu, Y. Li, G. Peng, J. Cai, L. Jin, L. Ma, H. Deng, M. Zeller, S. R. Batten, *Cryst. Growth Des.* **2010**, *10*, 1332–1340.

[17] S. Horike, S. Shimomura, S. Kitagawa, *Nat. Chem.* **2009**, *1*, 695–704.

[18] We have characterised by single-crystal X-ray diffraction eight MOFs with Zn (Table 1 and Table S5 in the Supporting Information) having the same network structure, in which the anions populate the channels (free or only weakly coordinated to Ag^+ ions), that exhibit *c*/*a* values from 1.11 to 1.04 and volumes from 3239 to 3550 $Å^3$ in response to the total channel content (not only due to the anion dimensions). We have observed variations of the channels, shrinkage of which, corresponding to reduction of the free voids, implies an increase of the *c*/*a* ratio. This would seem to be a possible deformation path and needs to be fully confirmed for this compound in future research.

[19] A. L. Spek, *J. Appl. Crystallogr.* **2003**, *36*, 7–13.

[20] S. Kitagawa, S. Noro, T. Nakamura, *Chem. Commun.* **2006**, 701–707.

[21] J.-P. Zhang, S. Horike, S. Kitagawa, *Angew. Chem.* **2007**, *119*, 907–910; *Angew. Chem. Int. Ed.* **2007**, *46*, 889–892.

[22] Due to the very poor solubility of these compounds in common solvents, it was not possible to establish the anion contents by direct solution NMR analyses. We have tried to quantify the amount of BF_4^- anions contained in the channels of the corresponding polymers by ^{19}F NMR spectroscopy of solutions obtained after exchange of ClO_4^- by BF_4^- (see text below), using trifluorotoluene as a standard. The experimental amounts of anions corresponded to almost the correct ratio. Elemental analyses of the crystals attempted by means of SEM showed only that the content of the channels is highly variable and can change from one crystal to another, as well as within the same crystal from one region to another. Hence, we can conclude that the composition of the channels is very changeable.

[23] a) To confirm the nature of the desolvation/resolvation process, a few single crystals of compound **4b** were desolvated in an oven at 100 °C for 30 min (see TGA in Figure S3 in the Supporting Information) and then left in air at room temperature. After these processes, the single crystallinity was maintained and the single-crystal X-ray diffraction pattern at room temperature yielded cell parameters of $a=b=15.72(5)$; $c=16.19(5)$ Å; $V=3476(12)$ $Å^3$. b) A few single crystals of compound **4b** were suspended in a saturated methanolic solution of $NaClO_4$ and the mixture was left under moderate shaking for 3 h. Observation of the crystals under an optical microscope revealed that they had retained their shape (see Figure S13 in the Supporting Information) and the IR spectrum obtained from a portion of this sample showed that BF_4^- had been exchanged by ClO_4^-. Single-crystal X-ray diffraction analysis of a few selected crystals at room temperature revealed that the single crystallinity had been preserved and that the cell parameters were very similar to the original ones for **4a**, for example, $a=b=15.53(6)$; $c=16.28(6)$ Å; $V=3400(12)$ $Å^3$. The same result was obtained after leaving the crystals in a saturated methanolic solution of $NaClO_4$ for 24 h.

[24] a) S. Kitagawa, M. Kondo, *Bull. Chem. Soc. Jpn.* **1998**, *71*, 1739–1753; b) K. Uemura, S. Kitagawa, M. Kondo, K. Fukui, R. Kitaura, H.-O. Chang, T. Mizutani, *Chem. Eur. J.* **2002**, *8*, 3586–3600; c) S. Kitagawa, R. Matsuda, *Coord. Chem. Rev.* **2007**, *251*, 2490–2509.

[25] C. Jiang, Y.-S. Wen, L.-K. Liu, T. S. A. Hor, Y. K. Yan, *Organometallics* **1998**, *17*, 173–181.

[26] J. J. Brunet, F. B. Kindela, D. Neibecker, S. A. Wander, M. Y. Darensbourg, *Inorg. Synth.* **1992**, *29*, 151–156.

[27] W. C. Fernelius, J. J. Burbage, *Inorg. Synth.* **1946**, *2*, 227–228.

[28] SADABS: Siemens Area Detector Absorption Correction Software, G. M. Sheldrick, University of Goettingen (Germany), **1996**.

[29] A. Altomare, M. C. Burla, M. Camalli, G. Cascarano, C. Giacovazzo, A. Guagliardi, A. G. Moliterni, G. Polidori, R. Spagna, *J. Appl. Crystallogr.* **1999**, *32*, 115–119.

[30] SHELX-97, G. M. Sheldrick, University of Goettingen (Germany), **1997**.

[31] L. J. Farrugia, *Appl. Crystallogr.* **1999**, *32*, 837–838.

[32] P. Van der Sluis, A. L. Spek, *Acta Crystallogr. Sect. A* **1990**, *46*, 194–201.

[33] L. J. Farrugia, *J. Appl. Crystallogr.* **1997**, *30*, 565.

[34] V. A. Blatov, *IUCr Comput. Comm. Newslett.* **2006**, *7*, 4, see also: http://www.topos.ssu.samara.ru.

[35] C. F. Macrae, P. R. Edgington, P. McCabe, E. Pidcock, G. P. Shields, R. Taylor, M. Towler, J. van de Streek, *J. Appl. Crystallogr.* **2006**, *39*, 453–457.

Received: May 10, 2010
Published online: October 11, 2010

